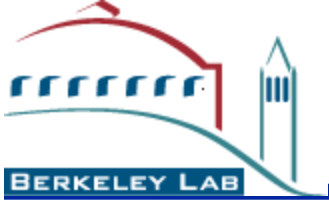


# Ge Charge-Coupled Device Development

LBNL LDRD project (3<sup>rd</sup> year)

Steve Holland, David Schlegel, Co Tran  
Lawrence Berkeley National Laboratory

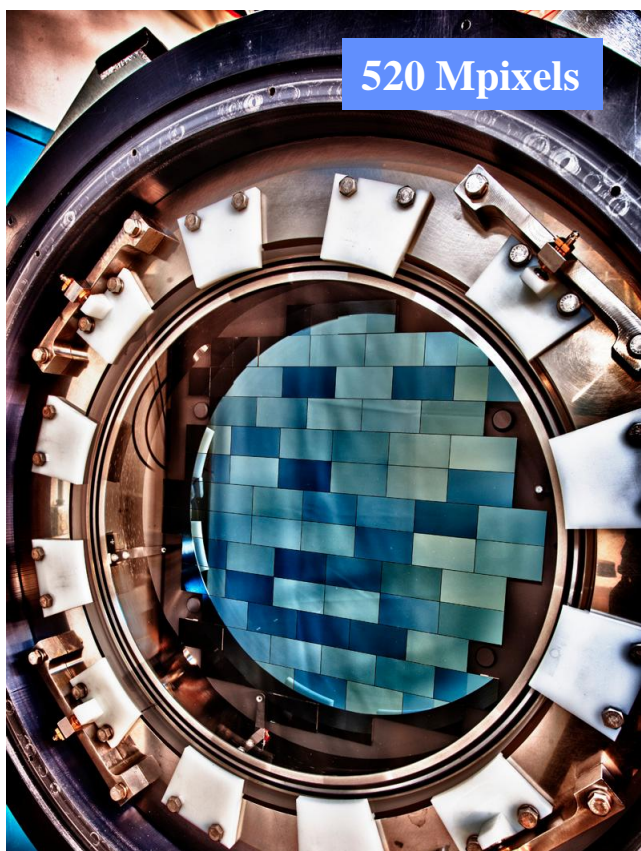
January 16<sup>th</sup>, 2019



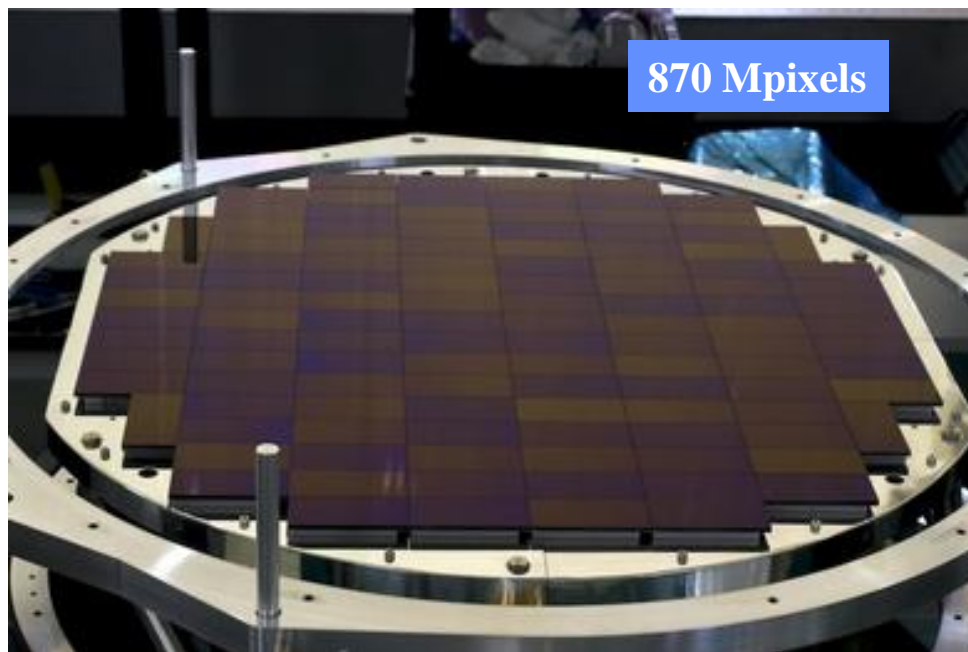
# LBNL Ge R&D (LDRD)

- This is an LDRD-funded effort to develop scientific CCDs on Germanium substrates
  - The next logical step in terms of increasing the long-wavelength response of scientific CCDs
    - ~ 10 - 20  $\mu\text{m}$  thick CCDs perform to  $\lambda \sim 700 \text{ nm}$
    - 250  $\mu\text{m}$  thick fully depleted CCDs  $\lambda \sim 1 \mu\text{m}$
    - Ge CCDs could work out to  $\lambda \sim 1.4 \mu\text{m}$
- Direct application to the study of high red-shift objects of interest in Dark Energy studies

## Examples of astronomical CCD cameras



FermiLab Dark Energy Survey Camera (DECam)  
62 2k x 4k,  $(15 \mu\text{m})^2$ -pixel CCDs  
CCDs from DALSA Semiconductor / LBNL  
*NOAO Cerro Tololo Blanco 4-m Telescope*



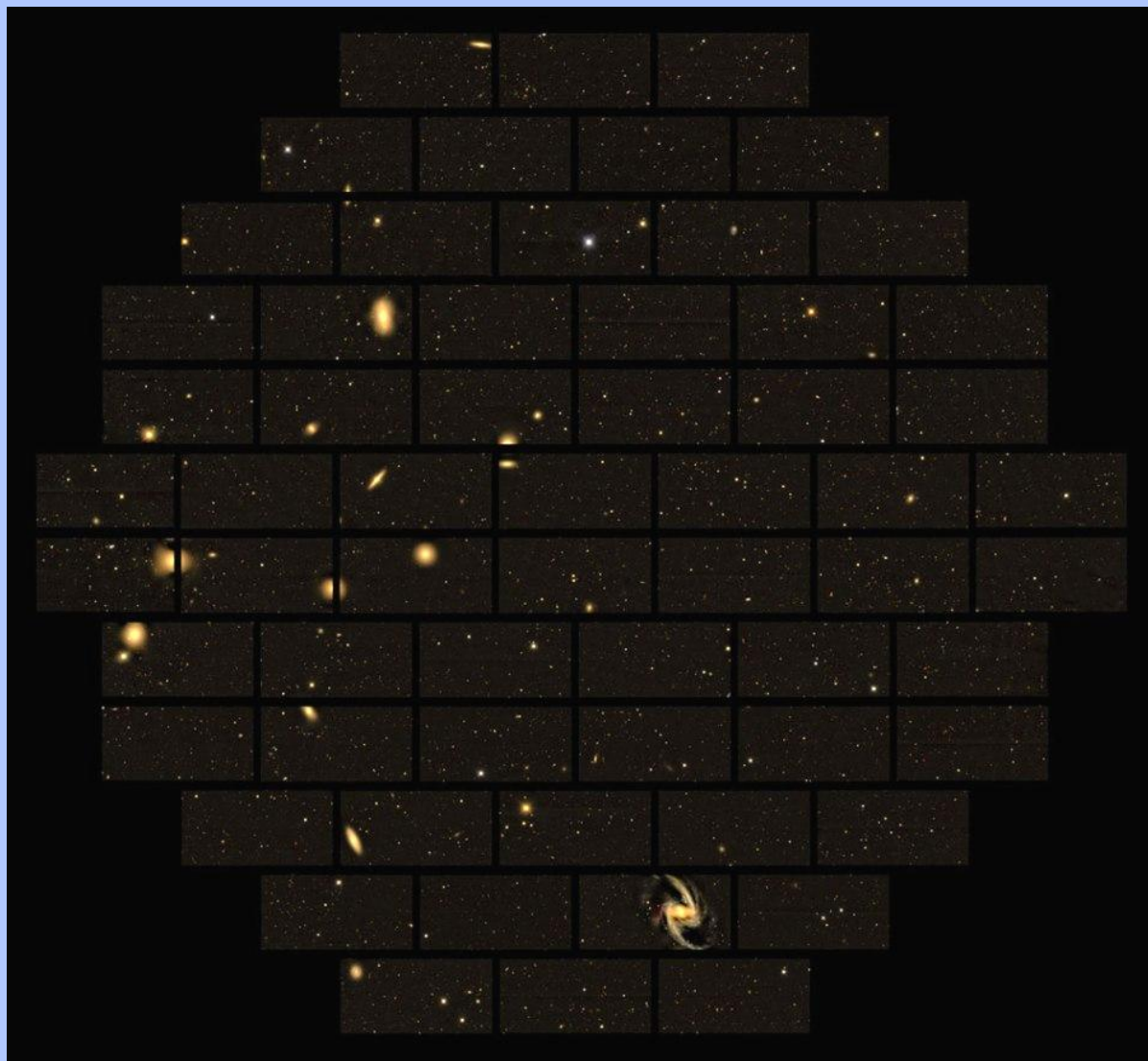
HyperSuprimeCam – 116 2k x 4k,  $(15 \mu\text{m})^2$ -pixel CCDs  
CCDs from Hamamatsu Corporation  
Licensed CCD technology from LBNL  
*Subaru 8-m Telescope*

Both use fully depleted CCDs (200 – 250  $\mu\text{m}$  thick)  
Operational since 2012

# Astronomical cameras with fully depleted CCDs

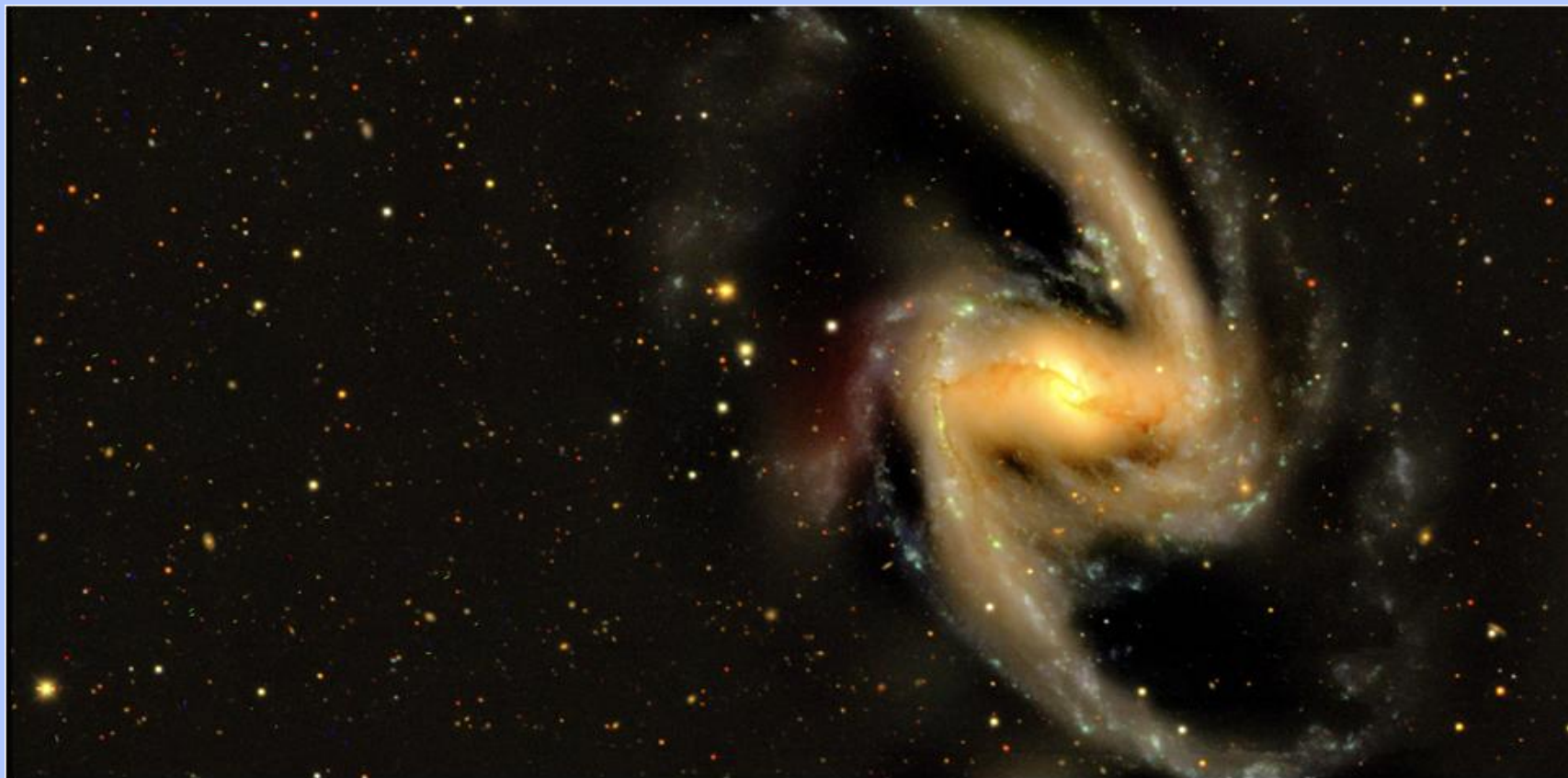


Full moon  
for scale



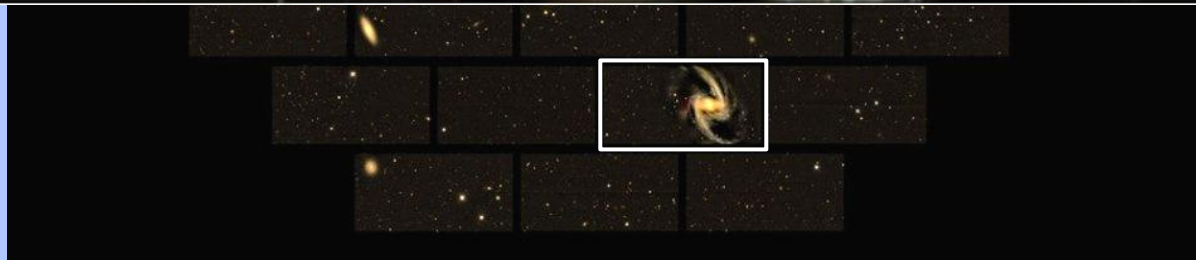
FermiLab Dark Energy Survey Camera (DECam)  
62 2k x 4k,  $(15 \mu\text{m})^2$ -pixel CCDs (520 Mpixels)  
*CCDs from DALSA Semiconductor / LBNL*

# Astronomical cameras with fully depleted CCDs



Roughly 50k galaxies per image

6 year DES survey complete as of last week / DECam remains



FermiLab Dark Energy Survey Camera (DECam)

62 2k x 4k,  $(15 \mu\text{m})^2$ -pixel CCDs (520 Mpixels)

CCDs from *DALSA Semiconductor / LBNL*

# M1/Crab Nebula in z band: “First and Last”



**Dark Energy Spectroscopic Instrument**  
U.S. Department of Energy Office of Science  
Lawrence Berkeley National Laboratory

MOSAIC 3 Camera / 500  $\mu\text{m}$  thick LBNL CCDs  
David Schlegel, Chris Bebek, Armin Karcher, Sufia Haque

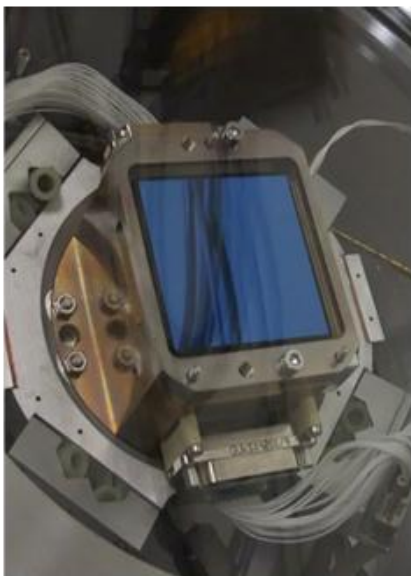
# Astronomical cameras with fully depleted CCDs



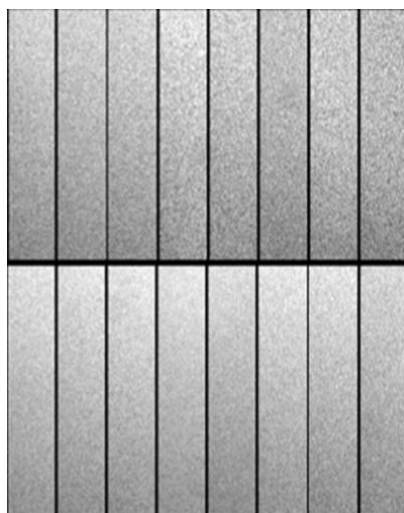
*HyperSuprimeCam – 8 degrees x 3 degrees field of view  
Video courtesy of Satoshi Miyazaki / Subaru Telescope*

# LSST CCDs (in production)

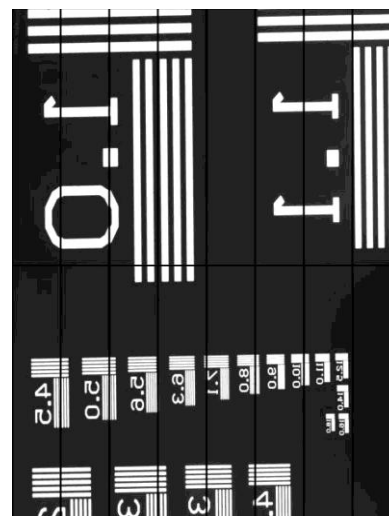
CCD in test fixture



Uniform illumination



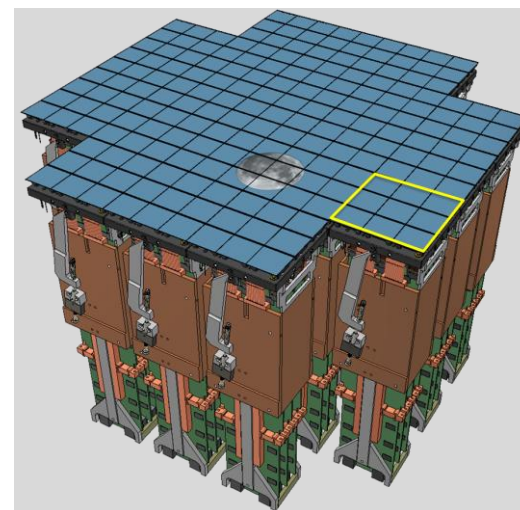
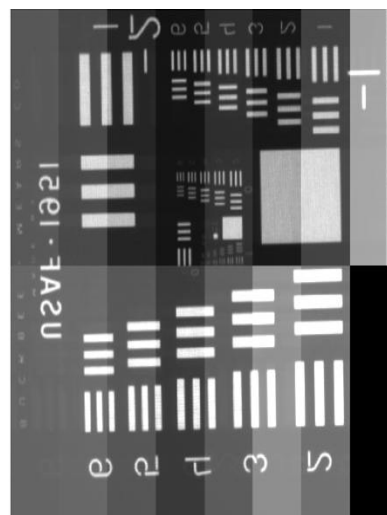
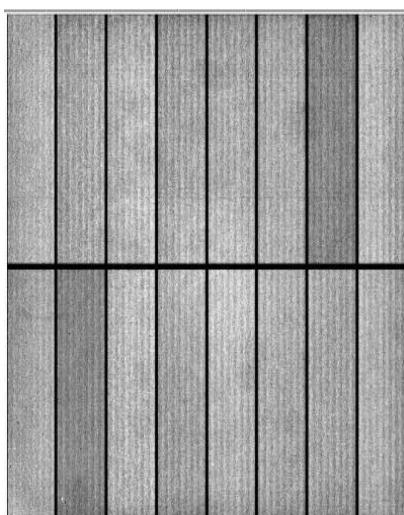
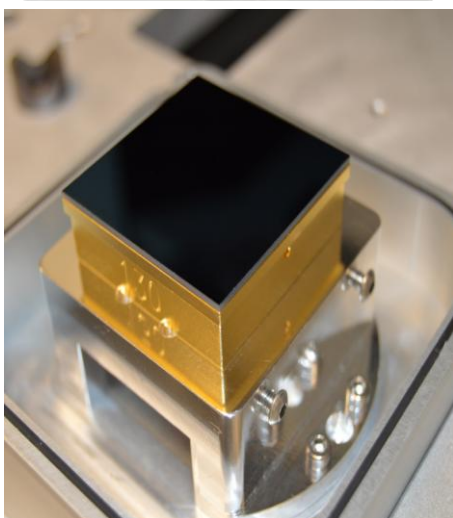
Test target image



- ❑ 100  $\mu\text{m}$  thick
- ❑ Fully depleted
- ❑ 4k x 4k
- ❑ 10  $\mu\text{m}$  pixels
- ❑ 16 amplifiers
  
- ❑ 189 CCDs
- ❑ 3.2 Gpixels

T-E2v CCD250

T-DALSA/ITL STA3800C







# LBNL Ge R&D (LDRD)

- In the following we compare material properties of silicon and germanium, and discuss how these material properties affect the electrical and optical performance

					2 <b>He</b> Helium 4.002602	
	5 <b>B</b> Boron 10.811	6 <b>C</b> Carbon 12.0107	7 <b>N</b> Nitrogen 14.0067	8 <b>O</b> Oxygen 15.9994	9 <b>F</b> Fluorine 18.9984032	10 <b>Ne</b> Neon 20.1797
	13 <b>Al</b> Aluminium 26.9815386	14 <b>Si</b> Silicon 28.0855	15 <b>P</b> Phosphorus 30.973762	16 <b>S</b> Sulfur 32.065	17 <b>Cl</b> Chlorine 35.453	18 <b>Ar</b> Argon 39.948
30 <b>Zn</b> Zinc 65.38	31 <b>Ga</b> Gallium 69.723	32 <b>Ge</b> Germanium 72.64	33 <b>As</b> Arsenic 74.92160	34 <b>Se</b> Selenium 78.96	35 <b>Br</b> Bromine 79.904	36 <b>Kr</b> Krypton 83.798
48 <b>Cd</b> Cadmium 112.411	49 <b>In</b> Indium 114.818	50 <b>Sn</b> Tin 118.710	51 <b>Sb</b> Antimony 121.760	52 <b>Te</b> Tellurium 127.60	53 <b>I</b> Iodine 126.90447	54 <b>Xe</b> Xenon 131.293

**Table 1. Comparison of some basic properties of Si, Ge, and GaAs at 300 K.**

Properties	Si	Ge	GaAs
Atoms/cm <sup>3</sup>	$5.02 \times 10^{22}$	$4.42 \times 10^{22}$	$4.42 \times 10^{22}$
Atomic weight	28.09	72.6	144.63
Breakdown field (V/cm)	$\sim 3 \times 10^5$	$\sim 1 \times 10^5$	$\sim 4 \times 10^5$
Crystal structure	Diamond	Diamond	Zincblende
Density (g/cm <sup>3</sup> )	2.329	5.326	5.317
Dielectric constant	11.9	16.0	13.1
Effective density of states in conduction band, $N_c$ (cm <sup>-3</sup> )	$2.86 \times 10^{19}$	$1.04 \times 10^{19}$	$4.7 \times 10^{17}$
Effective density of states in valance band, $N_v$ (cm <sup>-3</sup> )	$1.04 \times 10^{19}$	$6.0 \times 10^{18}$	$7.0 \times 10^{18}$
Optical phonon energy (eV)	0.063	0.037	0.035
Effective mass (conductivity)			
Electrons ( $m_n/m_0$ )	0.26	0.082	0.067
Holes ( $m_p/m_0$ )	0.69	0.28	0.57
Electron affinity, $\chi$ (V)	4.05	4.0	4.07
Energy gap (eV)	1.12	0.67	1.42
Intrinsic carrier concentration (cm <sup>-3</sup> )	$1.45 \times 10^{10}$	$2.4 \times 10^{13}$	$1.8 \times 10^6$
Intrinsic resistivity ( $\Omega$ -cm)	$2.3 \times 10^5$	47	$10^8$
Lattice constant ( $\text{\AA}$ )	5.431	5.646	5.653
Melting point ( $^{\circ}$ C)	1415	937	1240
Minority carrier lifetime (s)	$2.5 \times 10^{-3}$	$10^{-3}$	$\sim 10^{-8}$
Mobility (cm <sup>2</sup> /V·s)			
Electron ( $\mu_n$ )	1,500	3900	8,500
Holes ( $\mu_p$ )	450	1900	450
Thermal diffusivity (cm <sup>2</sup> /s)	0.9	0.36	0.24
Thermal conductivity (W/cm <sup>-2</sup> ·C)	1.5	0.6	0.46

## Properties of the semiconductors Si, Ge, and GaAs

Table 1. Comparison of some basic properties of Si, Ge, and GaAs at 300 K.

Properties	Si	Ge	GaAs
Atoms/cm <sup>3</sup>	5.02 × 10 <sup>22</sup>	4.42 × 10 <sup>22</sup>	4.42 × 10 <sup>22</sup>
Atomic weight	28.09	72.6	144.63
Breakdown field (V/cm)	~ 3 × 10 <sup>5</sup>	~ 1 × 10 <sup>5</sup>	~ 4 × 10 <sup>5</sup>

Table 1. Comparison of some basic properties of Si, Ge, and GaAs at 300 K.

Properties	Si	Ge
Energy gap (eV)	1.12	0.67

Effective mass (conductivity)

Electrons ( $m_n/m_o$ )

Holes ( $m_p/m_o$ )

Electron affinity,  $\chi$  (V)

Energy gap (eV)

Intrinsic carrier concentration (cm<sup>-3</sup>)

Intrinsic resistivity ( $\Omega$ -cm)

Lattice constant (Å)

Melting point (°C)

Minority carrier lifetime (s)

Mobility (cm<sup>2</sup>/V·s)

Electron ( $\mu_n$ )

Holes ( $\mu_p$ )

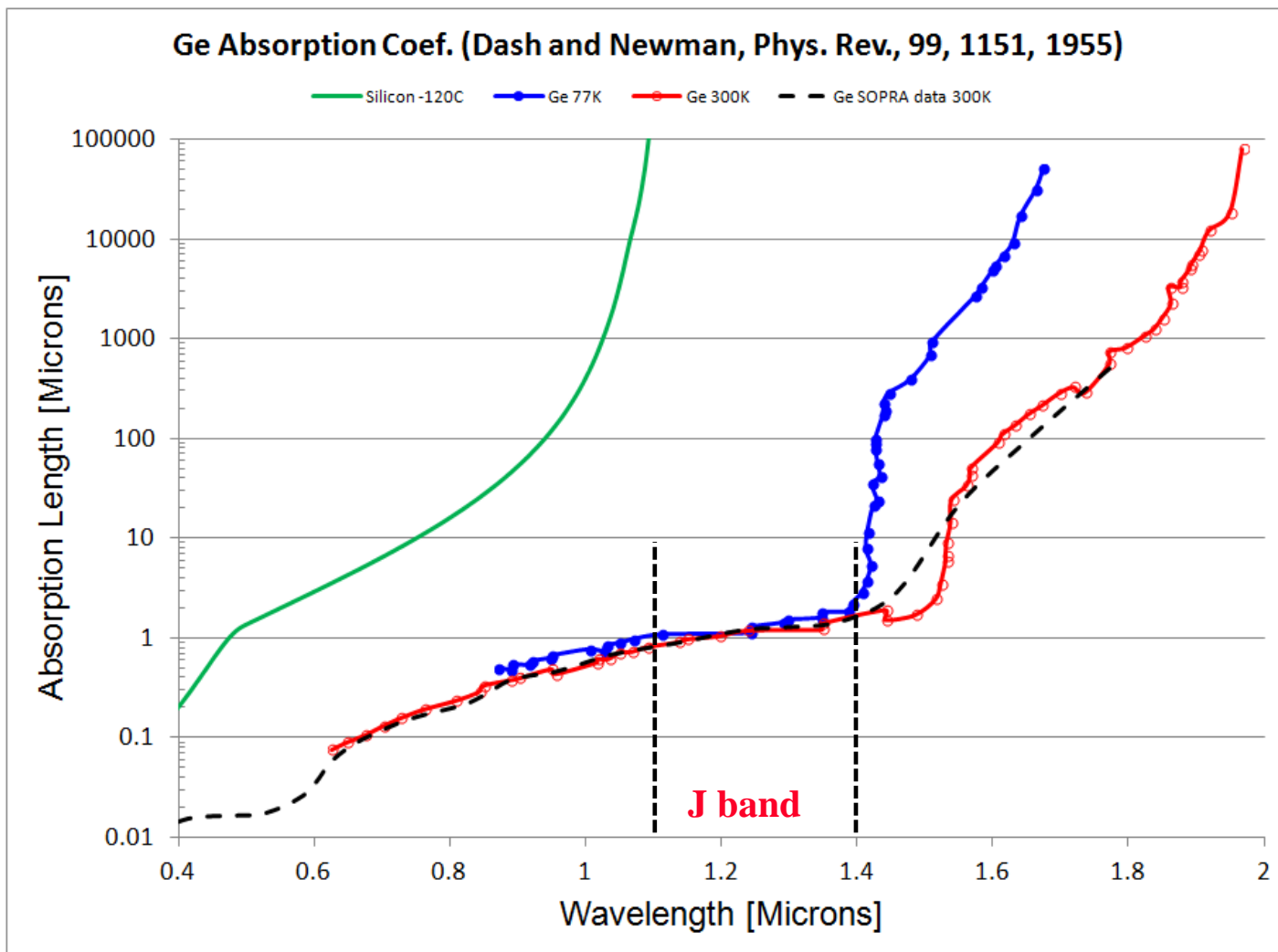
Thermal diffusivity (cm<sup>2</sup>/s)

Thermal conductivity (W/cm<sup>2</sup>·C)

$$\lambda_{cutoff} \approx \frac{1.24}{E_g}$$

0.82	0.067
0.28	0.57
0.40	4.07
1.12	1.42
1.0 × 10 <sup>13</sup>	1.8 × 10 <sup>6</sup>
10 <sup>7</sup>	10 <sup>8</sup>
3.56	5.653
1415	937
2.5 × 10 <sup>-3</sup>	10 <sup>-3</sup>
~ 10 <sup>-8</sup>	
1,500	3900
8,500	
450	1900
450	
0.9	0.36
0.24	
1.5	0.6
0.46	

# Germanium vs Silicon



- Higher redshifts, e.g.  $z = 1.6$  to  $2.6$  for DESI [O II] (Si to Ge)
  - 2x volume reach for future DESI with Ge CCDs

Table 1. Comparison of some basic properties of Si, Ge, and GaAs at 300 K.

Properties	Si	Ge	GaAs
Atoms/cm <sup>3</sup>	5.02 × 10 <sup>22</sup>	4.42 × 10 <sup>22</sup>	4.42 × 10 <sup>22</sup>
Atomic weight	28.09	72.6	144.63
Breakdown field (V/cm)	~ 3 × 10 <sup>5</sup>	~ 1 × 10 <sup>5</sup>	~ 4 × 10 <sup>5</sup>

Table 1. Comparison of some basic properties of Si, Ge, and GaAs at 300 K.

Properties	Si	Ge
Atomic weight	Z = 14 28.09	Z = 32 72.6
Density (g/cm <sup>3</sup> )	2.329	5.326

Holes (m <sub>p</sub> /m <sub>0</sub> )	0.69	0.28	0.57
---	------	------	------

Ge is 2.3x denser than silicon  
 Good for  $\gamma$  and x-ray detection  
 Practical issue: wafers are heavy

Mobility (cm <sup>2</sup> /V·s)			
Electron ( $\mu_n$ )	1,500	3900	8,500
Holes ( $\mu_p$ )	450	1900	450
Thermal diffusivity (cm <sup>2</sup> /s)	0.9	0.36	0.24
Thermal conductivity (W/cm <sup>2</sup> ·C)	1.5	0.6	0.46

# $\gamma$ and x-ray Absorption vs Energy / Ge and Si

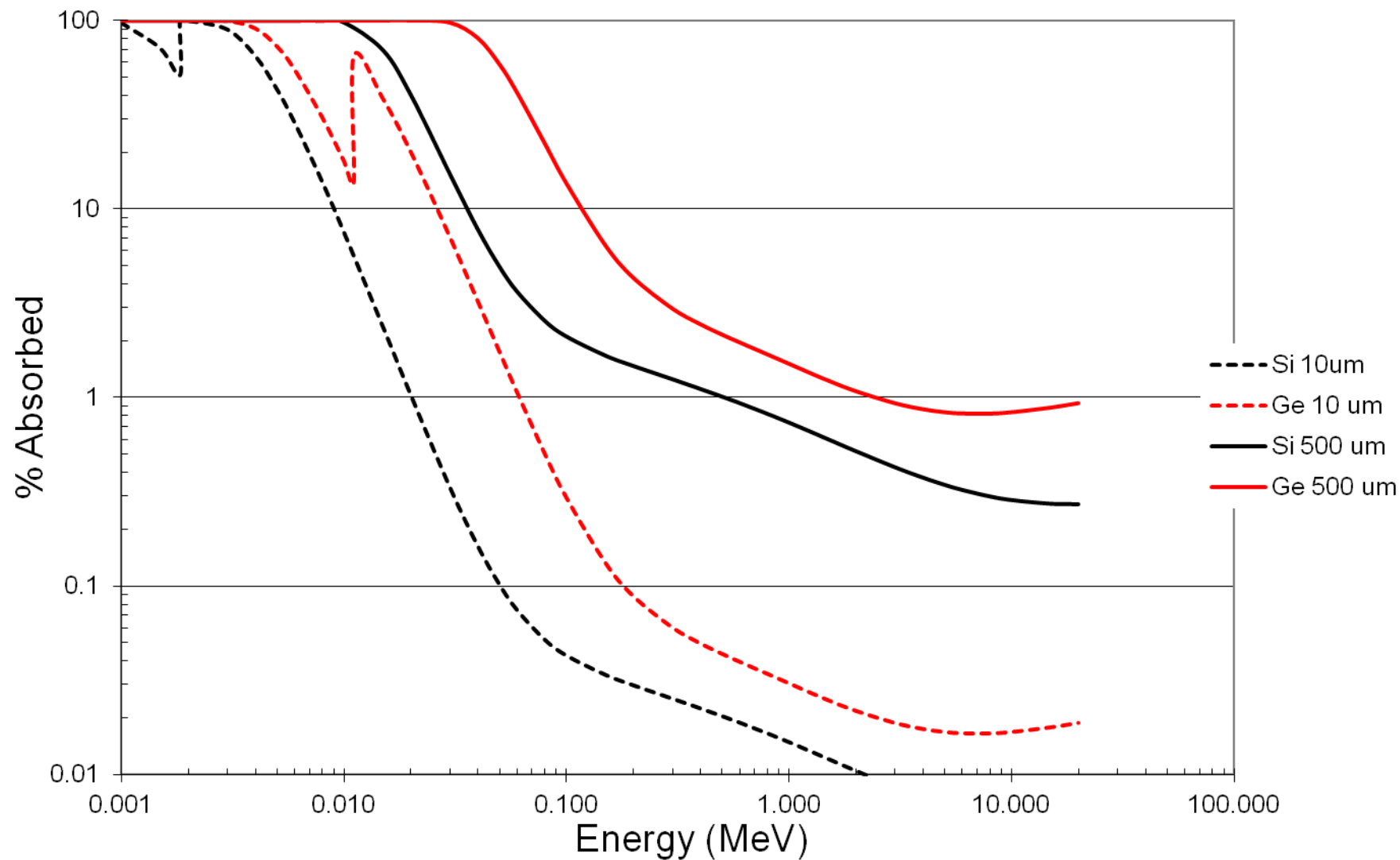


Table 1. Comparison of some basic properties of Si, Ge, and GaAs at 300 K.

Properties	Si	Ge	GaAs
Atoms/cm <sup>3</sup>	5.02 × 10 <sup>22</sup>	4.42 × 10 <sup>22</sup>	4.42 × 10 <sup>22</sup>
Atomic weight	28.09	72.6	144.63
Breakdown field (V/cm)	~ 3 × 10 <sup>5</sup>	~ 1 × 10 <sup>5</sup>	~ 4 × 10 <sup>5</sup>

Table 1. Comparison of some basic properties of Si, Ge, and GaAs at 300 K.

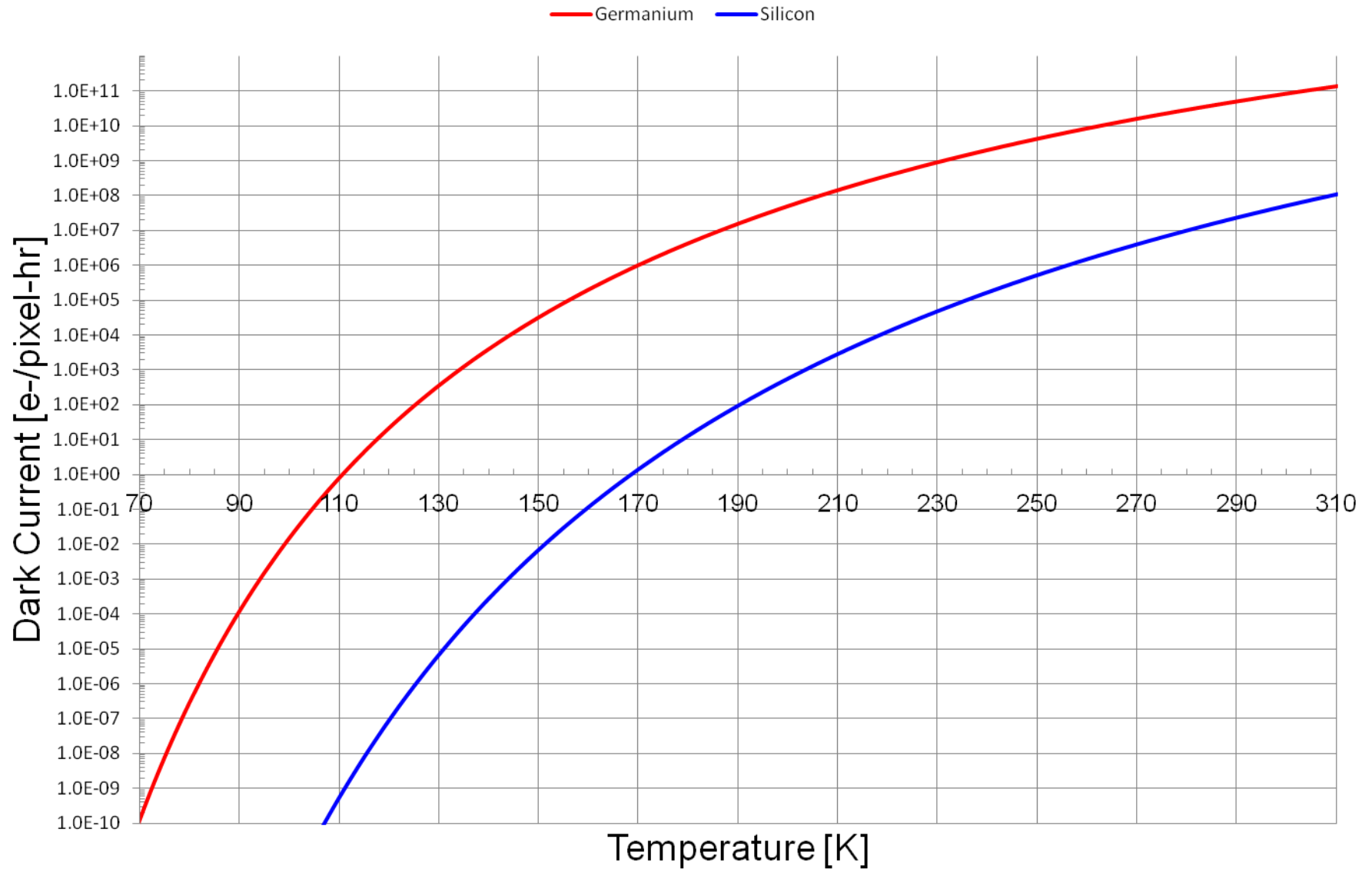
Properties	Si	Ge
Energy gap (eV)	1.12	0.67
Intrinsic carrier concentration (cm <sup>-3</sup> )	1.45 × 10 <sup>10</sup>	2.4 × 10 <sup>13</sup>
Minority carrier lifetime (s)	2 × 10 <sup>-3</sup>	10 <sup>-3</sup>

Holes (m <sub>p</sub> /m <sub>0</sub> )	0.69	0.28	0.57
---	------	------	------

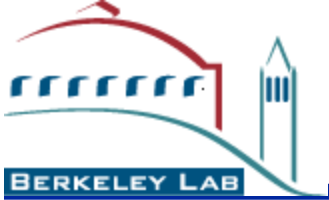
$$J_{leakage} \propto \frac{n_i}{\tau_g} \propto \frac{\exp(-E_g/2kT)}{\tau_g}$$

Mobility (cm <sup>2</sup> /V·s)			
Electron (μ <sub>n</sub> )	1,500	3900	8,500
Holes (μ <sub>p</sub> )	450	1900	450
Thermal diffusivity (cm <sup>2</sup> /s)	0.9	0.36	0.24
Thermal conductivity (W/cm <sup>2</sup> ·C)	1.5	0.6	0.46

Idealized calculated dark current / Si vs Ge  
Assumptions: Silicon forced to 1 nA/cm<sup>2</sup> at 300K, same  $\tau_g$  for both

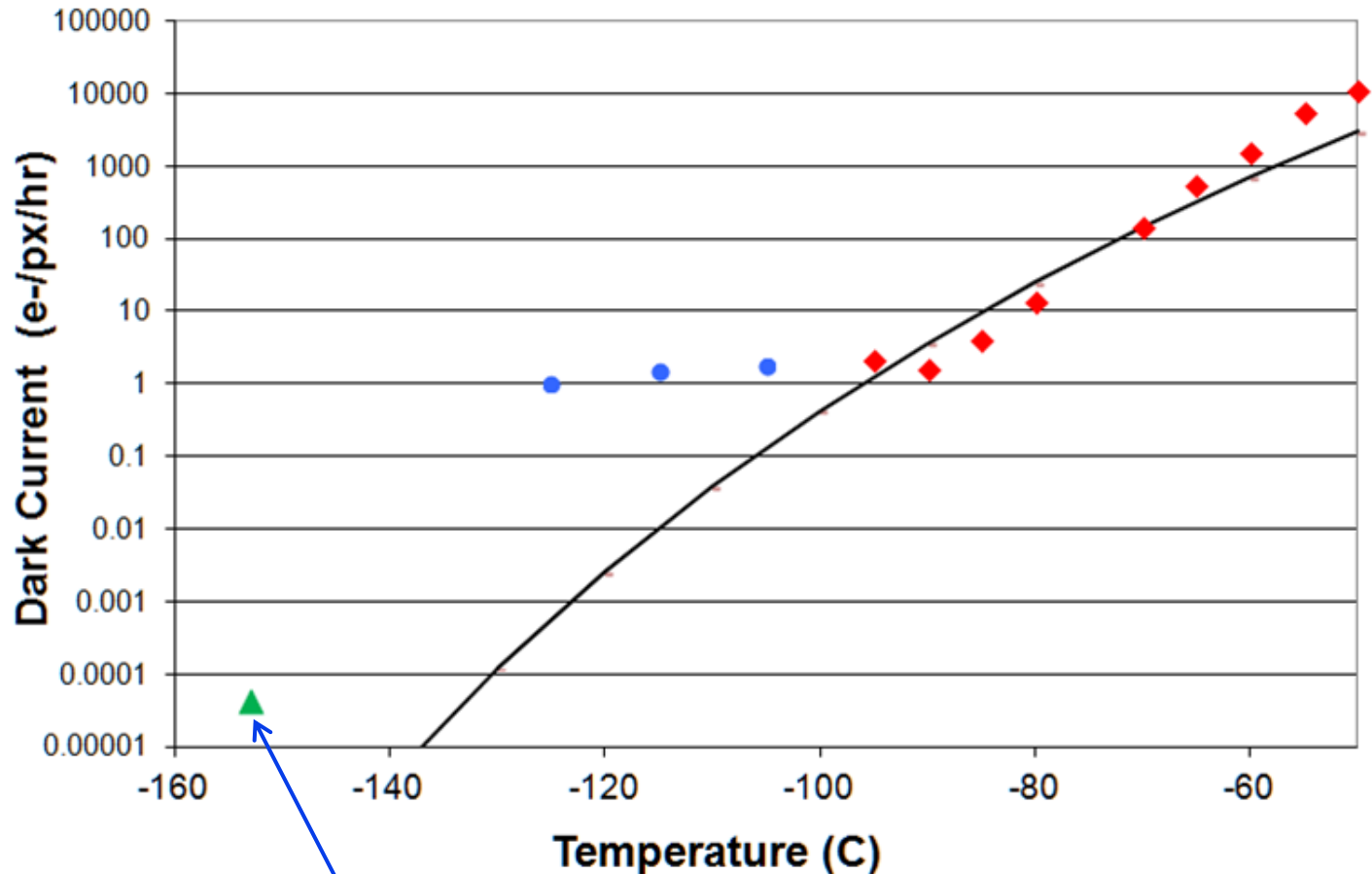






# LBNL CCD Dark Current

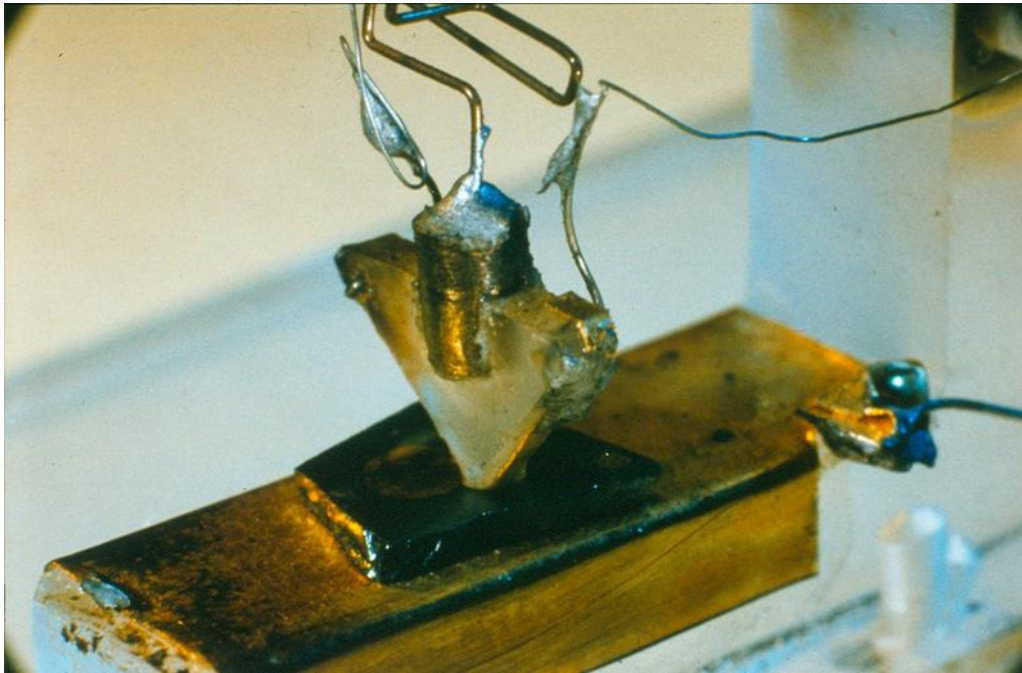
CCD Dark Current vs Temperature  
LBNL Fully Depleted CCD  
Measurements by Bill Kolbe



DAMIC roughly here with their cooled Cu box enclosure  
0.001 e- / pixel-day at 120K ( $4 \times 10^{-5}$  e- / pixel-hr)

# Very brief transistor history

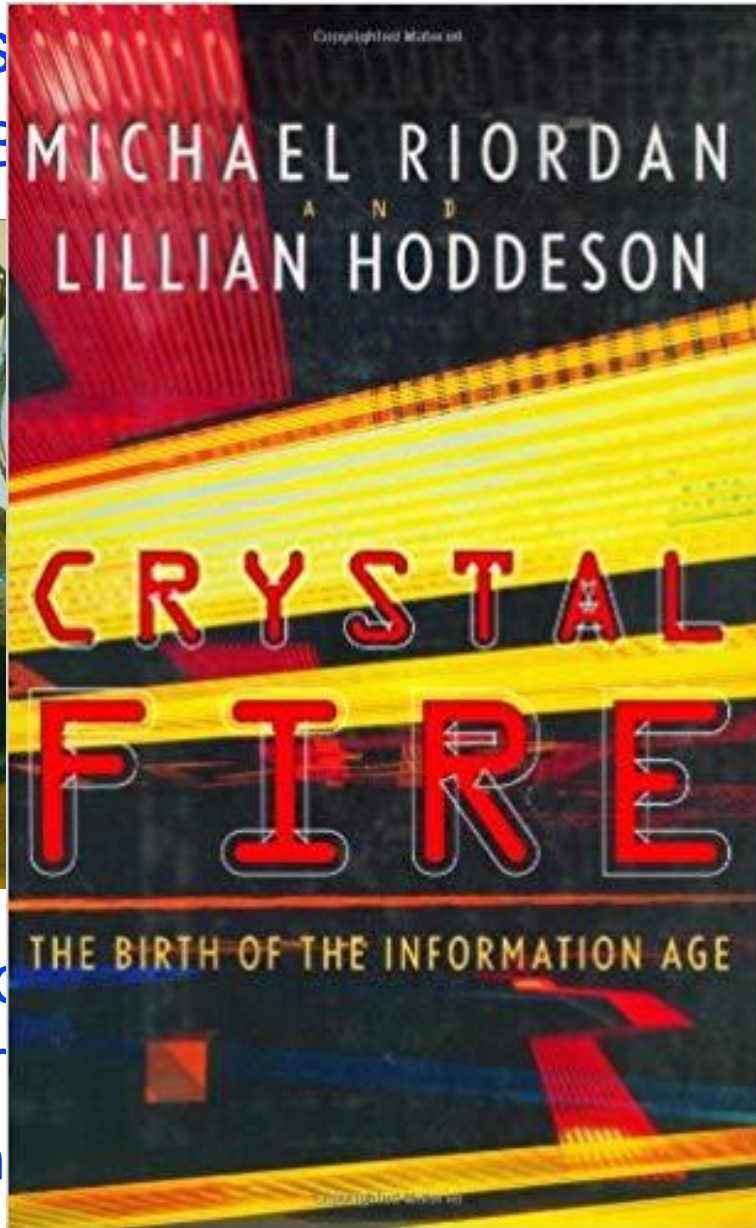
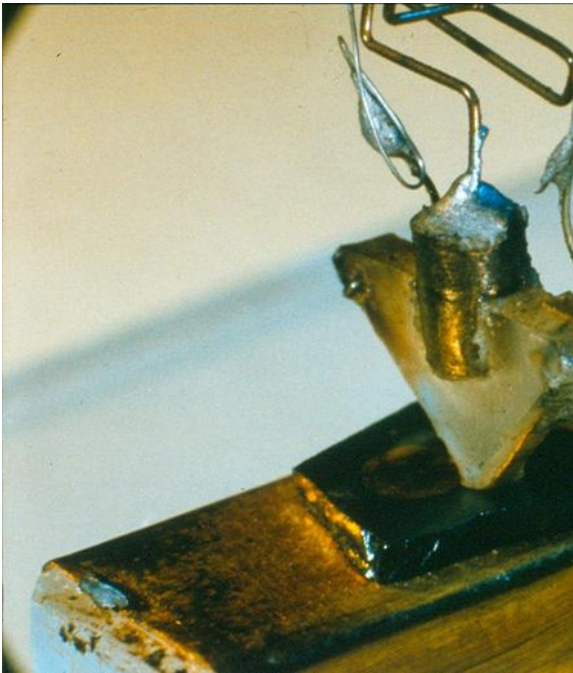
- The first transistor was realized in Ge (Dec. 1947)
  - Bardeen and Brattain, then Shockley's junction transistor



- 1<sup>st</sup> Ge transistor
  - Point contact
  - Ge because the purification process was more advanced than that for silicon due to the lower melting point of Ge
    - 937°C vs 1415°C (Si)
- At a 1954 IRE conference Texas Instruments demonstrates the silicon grown junction transistor
  - Ge and Si transistors in an audio amplifier dunked in hot oil

# Very brief transistor history

- The first transistor  
— Bardeen and E



- (Dec. 1947)  
unction transistor  
transistor  
nt contact  
cause the  
ation process was  
advanced than that  
con due to the  
melting point of Ge  
7°C vs 1415°C (Si)  
ents demonstrates  
r dunked in hot oil

- At a 1954 IRE conference  
the silicon grown  
— Ge and Si trans

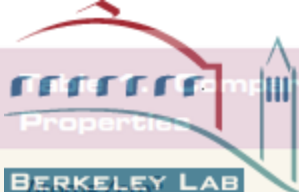


Table 1. Comparison of some basic properties of Si, Ge, and GaAs at 300 K.

Properties	Si	Ge	GaAs
Atomic weight	28.09	72.6	144.63
Breakdown field (V/cm)	$\sim 3 \times 10^5$	$\sim 1 \times 10^5$	$\sim 4 \times 10^5$

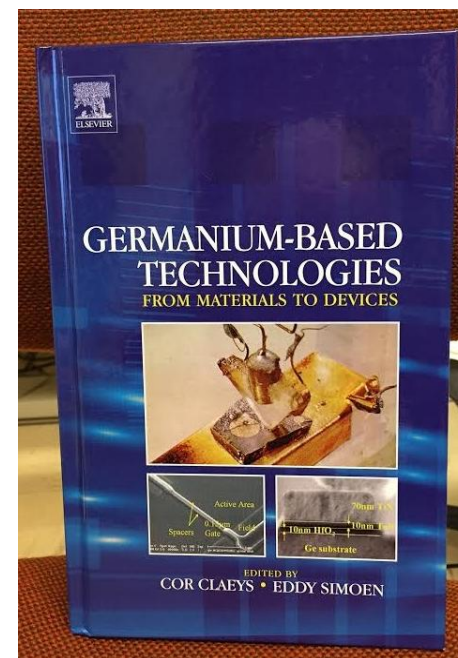
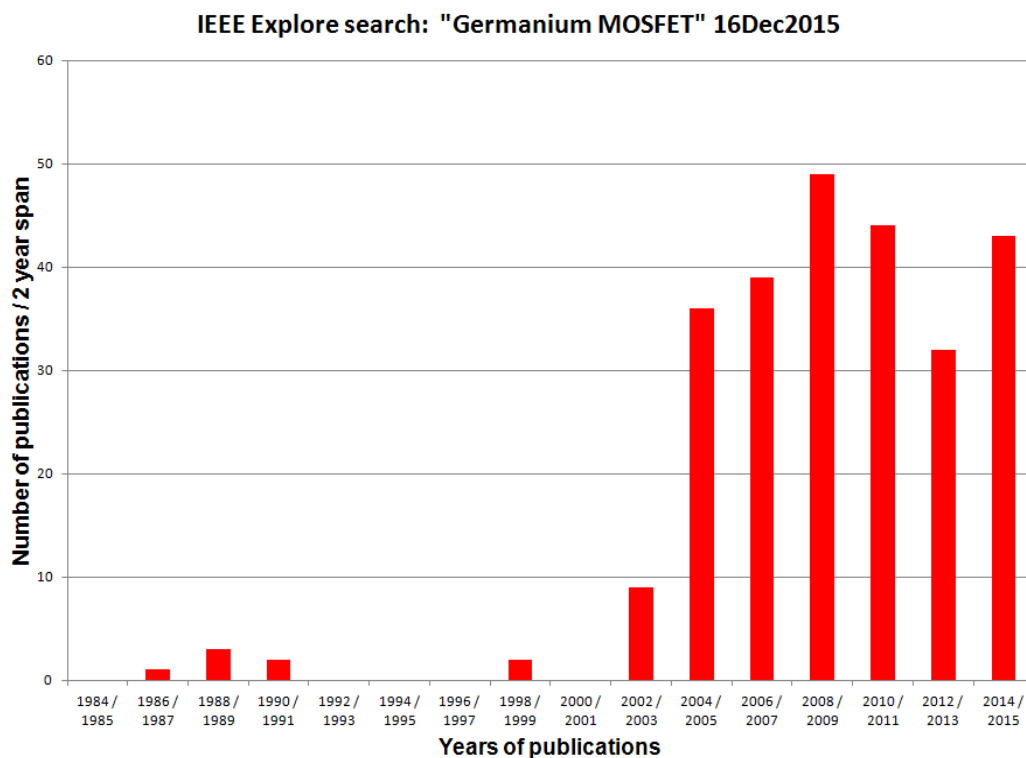
Table 1. Comparison of some basic properties of Si, Ge, and GaAs at 300 K.		
Properties	Si	Ge
Mobility (cm <sup>2</sup> /V·s)		
Electron ( $\mu_n$ )	1,500	3900
Holes ( $\mu_p$ )	450	1900

Holes ( $m_p/m_0$ )	0.69	0.28	0.57
Electron ( $m_n/m_0$ )	0.35	0.12	0.07
Energy band gap (eV)	1.12	0.66	1.42
Intrinsic carrier concentration (cm <sup>-3</sup> )	1.5 × 10 <sup>10</sup>	2.5 × 10 <sup>13</sup>	2 × 10 <sup>16</sup>
Intrinsic carrier lifetime (s)	10 <sup>-8</sup>	10 <sup>-8</sup>	10 <sup>-8</sup>
Lattice constant (Å)	357	357	357
Melting point (°C)	1414	938	1238
Minority carrier lifetime (s)	10 <sup>-8</sup>	10 <sup>-8</sup>	10 <sup>-8</sup>
Mobility (cm <sup>2</sup> /V·s)			
Electron ( $\mu_n$ )	1,500	3900	8,500
Holes ( $\mu_p$ )	450	1900	450
Thermal diffusivity (cm <sup>2</sup> /s)	0.9	0.36	0.24
Thermal conductivity (W/cm <sup>2</sup> ·C)	1.5	0.6	0.46

Germanium has high carrier mobilities  
 Ge has the largest hole mobility of any semiconductor

# Opportune time for Ge R&D

- Renewed interest in Ge due to high mobilities



- Umicore produces 150 and 200 mm Ge wafers (low resistivity) for mostly photovoltaic applications
- Ge CCD effort at M.I.T. Lincoln Laboratories



# Opportune time for Ge R&D

IEEE Explore search: "Germanium MOSFET" 16Dec2015

Do NOT Distribute

## Laboratory Directed Research and Development Program Berkeley Lab FY 2000 Coversheet

Project Title: Exploration of Technologies for Germanium CCD Imagers

Investigator(s): S. Holland, D. Groom, M. Levi, S. Perlmutter

Division: Physics

Funds Requested (FY 2000): \$60K

Proposed Project Duration: 1 year

Out Year Funds Requested:  
(for multiyear projects only)  
Continuation

New Proposal

Long-Term Funding (amount, source): NASA, NSF

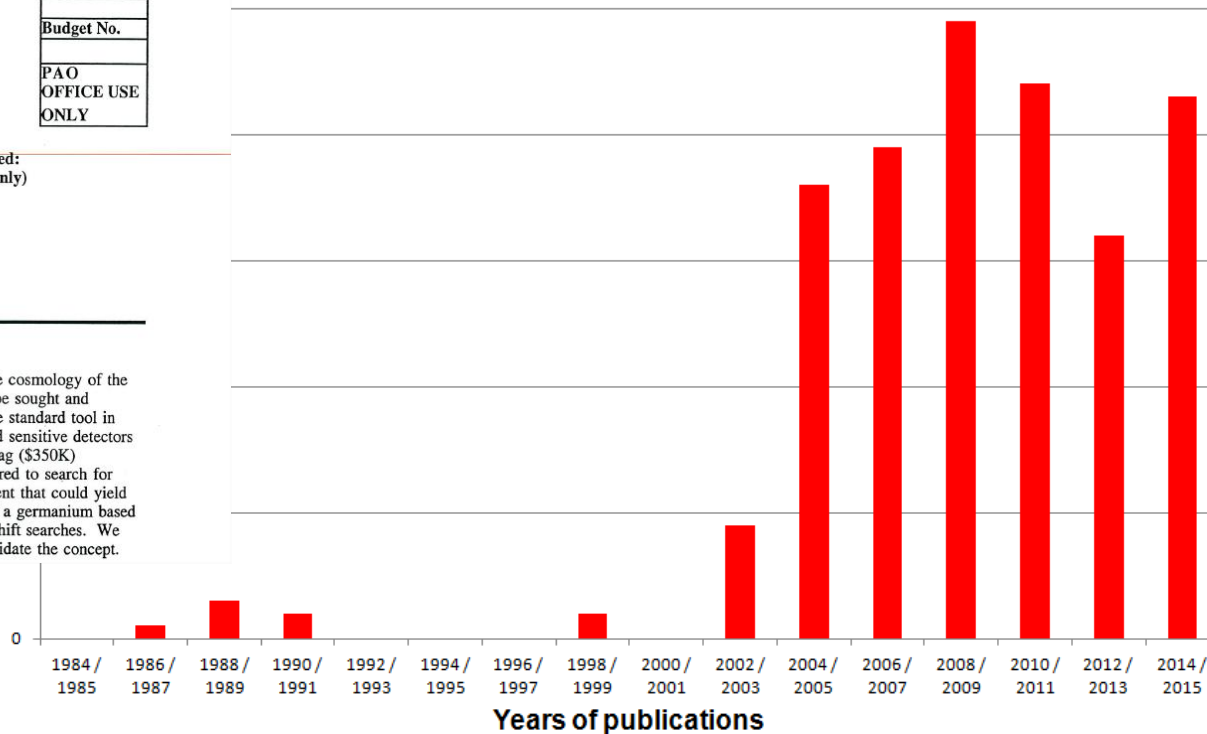
Collaborating Divisions or Institutions: Engineering

Prop No.
Budget No.
PAO OFFICE USE ONLY

### Summary

#### Purpose /Goals:

The search for high redshift supernova have led to a deeper understanding of the cosmology of the universe. In order to carry this work further even higher red-shift objects must be sought and characterized. Unfortunately, silicon CCD (charged-coupled device) imagers, the standard tool in astronomy, have no sensitivity beyond the silicon band-gap at 1050 nm. Infrared sensitive detectors such as InSb are available but only exist in small formats (1Kx1K) with a price-tag (\$350K) prohibiting the use of the technology for large area mosaic imaging arrays required to search for very distant supernova. We propose here a very high-risk technology development that could yield fantastic scientific benefits in astronomy and other applications. The creation of a germanium based CCD would be an ideal IR sensitive device (600 nm - 1500 nm) for the high redshift searches. We propose performing the early and critical process technology steps needed to validate the concept.



We applied for a Ge CCD LDRD in 2000  
Luckily it was not approved

- Numerous technical challenges with Ge
  - Water soluble  $\text{GeO}_2$  insulator that degrades starting at  $400^\circ\text{C}$  due to  $\text{GeO}_2$  decomposition (more on this later)

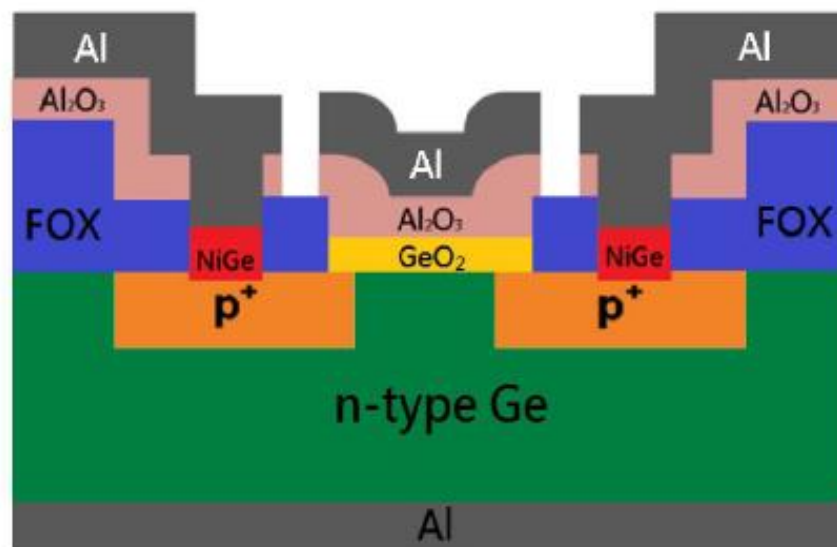
## Stabilization of the $\text{GeO}_2/\text{Ge}$ Interface by Nitrogen Incorporation in a One-Step NO Thermal Oxynitridation

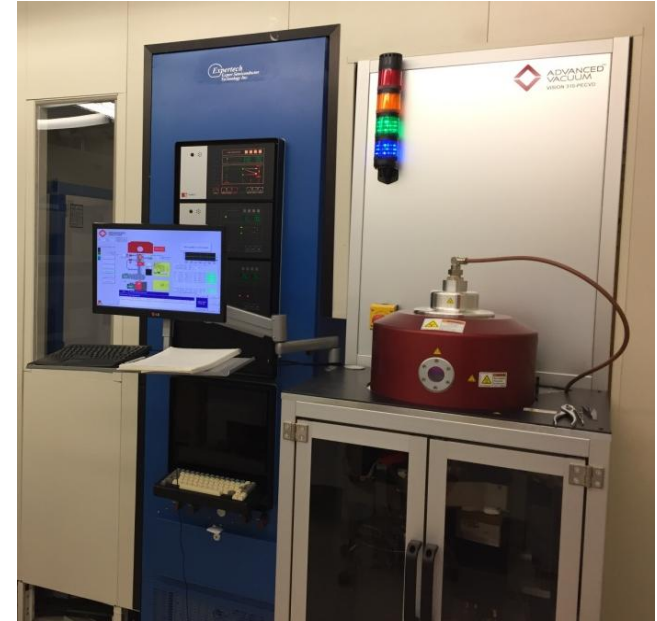
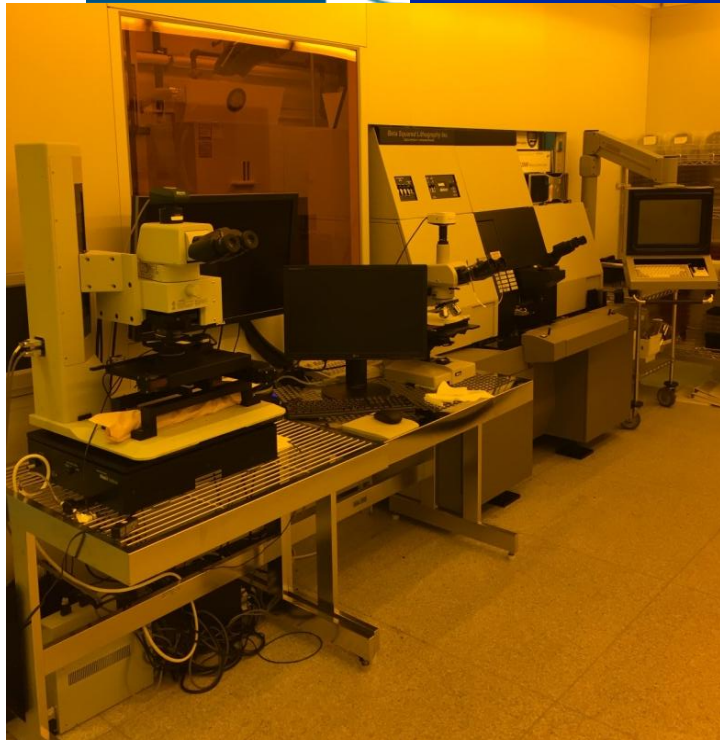
Gabriela Copetti,<sup>†</sup> Gabriel V. Soares,<sup>†</sup> and Cláudio Radtke<sup>\*,‡</sup>

<sup>†</sup>Instituto de Física and <sup>‡</sup>Instituto de Química, UFRGS, 91509-900 Porto Alegre, Brazil

However, the lack of a stable passivation layer for Ge surface hinders the development of such technology. Unlike silicon dioxide ( $\text{SiO}_2$ ), germanium dioxide ( $\text{GeO}_2$ ) is water-soluble and also thermally unstable at temperatures usually employed during device processing.<sup>2</sup> This instability is due to the interfacial reaction  $\text{GeO}_2 + \text{Ge} \rightarrow 2\text{GeO}$  that occurs at temperatures greater than  $400^\circ\text{C}$ . Oxygen vacancies generated at the  $\text{GeO}_2/\text{Ge}$  interface diffuse through the oxide toward the surface, where they promote  $\text{GeO}$  desorption (as evidenced by thermal desorption spectroscopy<sup>3</sup>), leading to the deterioration of the device's electrical properties.<sup>4</sup> First-principles calculations predicted that

- Nonetheless,  $\text{GeO}_2/\text{Ge}$  interface is better than the alternatives, so cap with another insulator

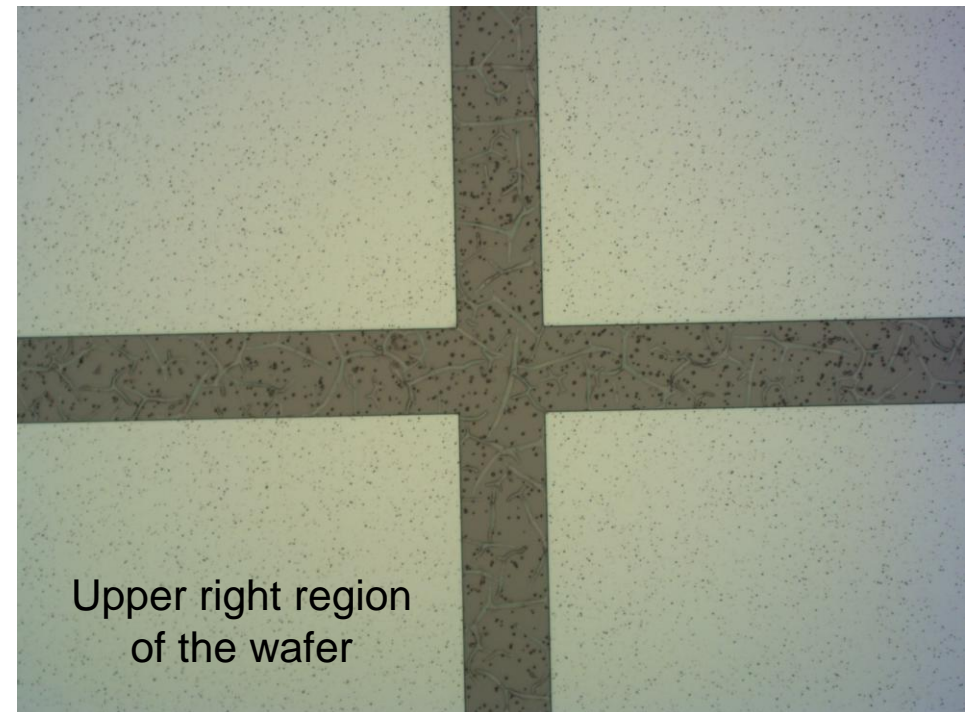
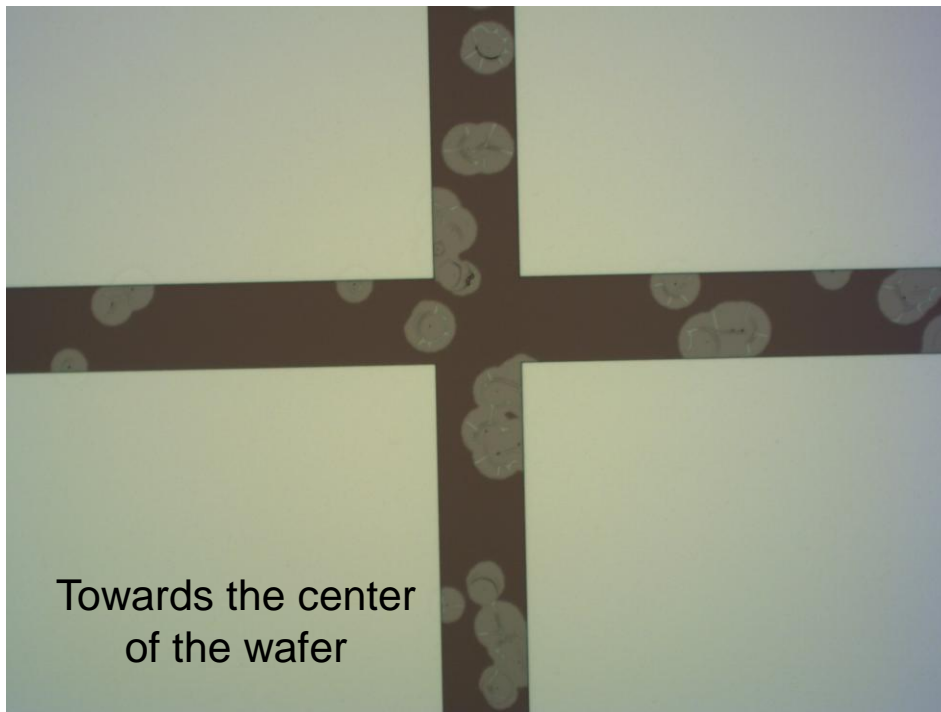




- Class 10 clean room
  - 150 mm wafer processing
  - DECam / DESI CCDs with DALSA
  - Ge CCD R&D

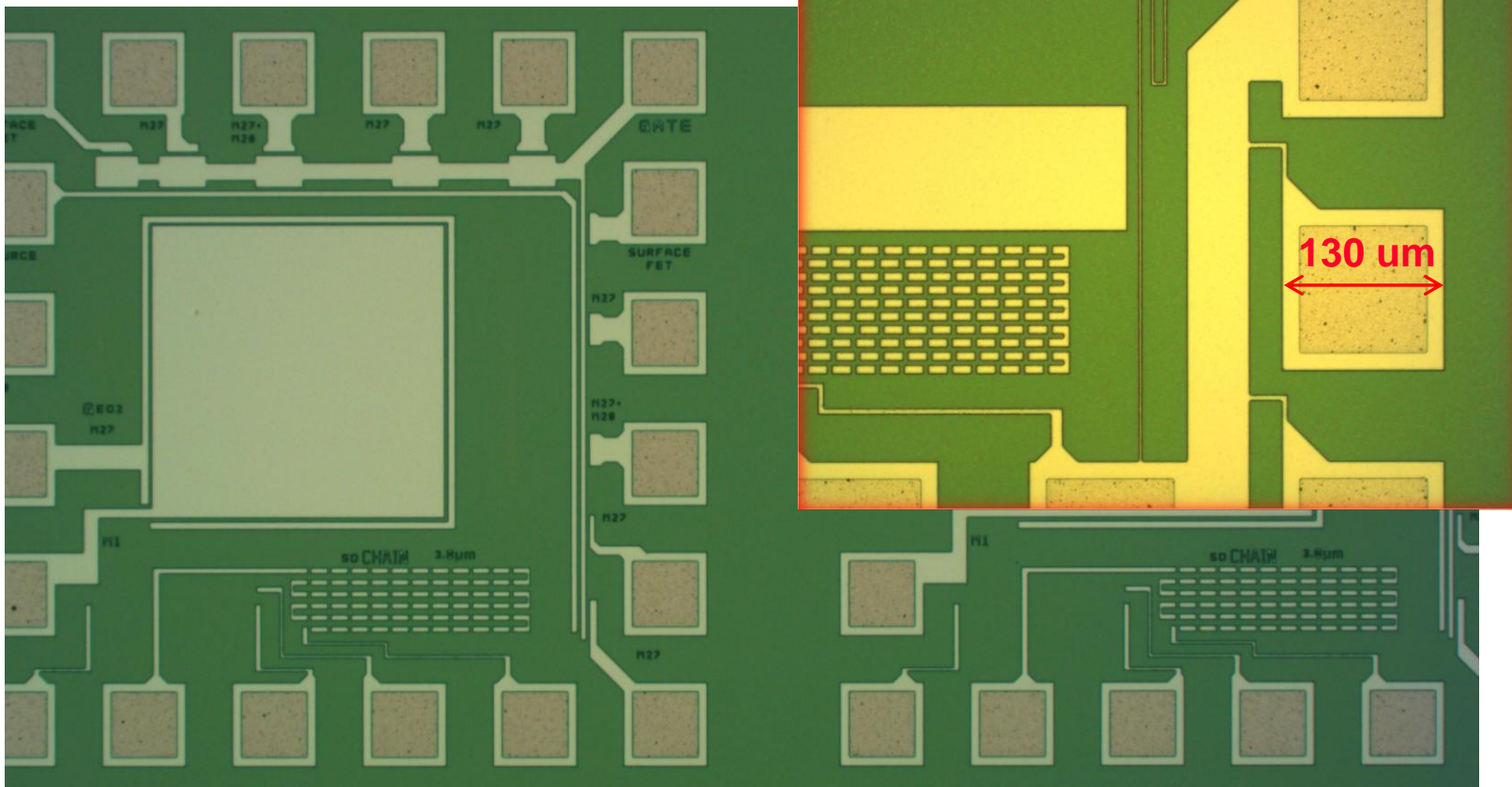


- 1<sup>st</sup> attempt at  $\text{GeO}_2$ - $\text{SiO}_2$  gate insulator
  - Low temperature ( $300^\circ\text{C}$ )  $\text{SiO}_2$  deposition over  $\text{GeO}_2$ 
    - Pinholes in the deposited  $\text{SiO}_2$  result in etching of the water-soluble  $\text{GeO}_2$  when exposed to e.g.  $\text{H}_2\text{O}$



Capacitor-only wafer: Aluminum over  $\text{SiO}_2$  over  $\text{GeO}_2$

- 2<sup>nd</sup> attempt at  $\text{SiO}_2$ - $\text{GeO}_2$  using improved methods
  - Two step  $\text{SiO}_2$  deposition / pinholes not likely coincident
  - Other improvements

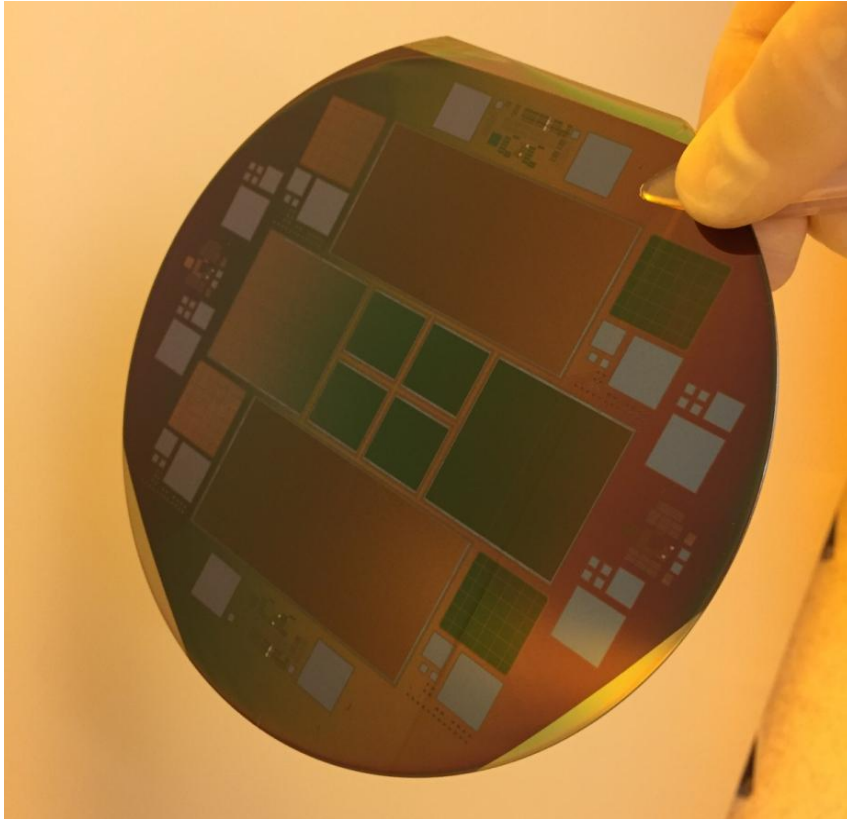


Capacitor-only wafer: Entire region is  $\text{SiO}_2$  over  $\text{GeO}_2$

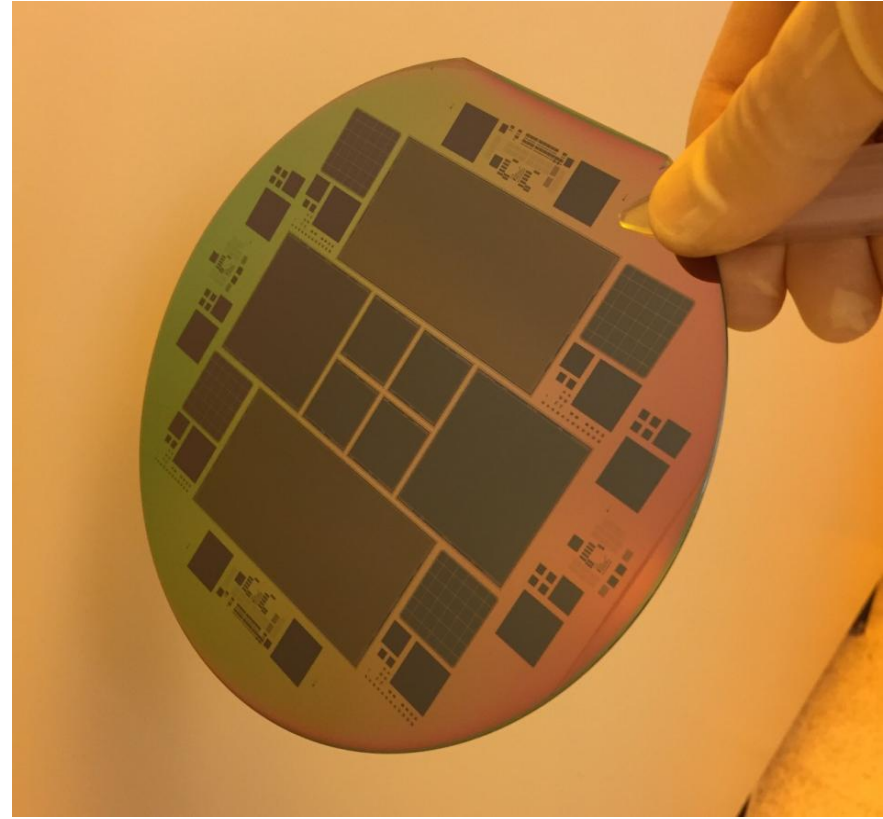


# LBNL Ge R&D (LDRD)

- Next step: Fabricate Ge buried-channel MOSFETs
  - Basic building block of CCDs
- Short-loop study to debug the basic Ge process
  - Metal gate transistors now, future polyGe gate
- Required two ion implantation steps
  - Work with implant vendor Innovion regarding their concerns with heavy / fragile Ge substrates
- Required MSL equipment upgrade for photoresist removal after high-dose implants
  - $\text{H}_2\text{SO}_4\text{-H}_2\text{O}_2$  often used in silicon not compatible with Ge (as is the case with most silicon cleans)



Post high-dose implant with resist mask



After plasma resist strip (previously unused "asher" outfitted with special wafer handler)

- Buried channel MOSFETs for CCDs

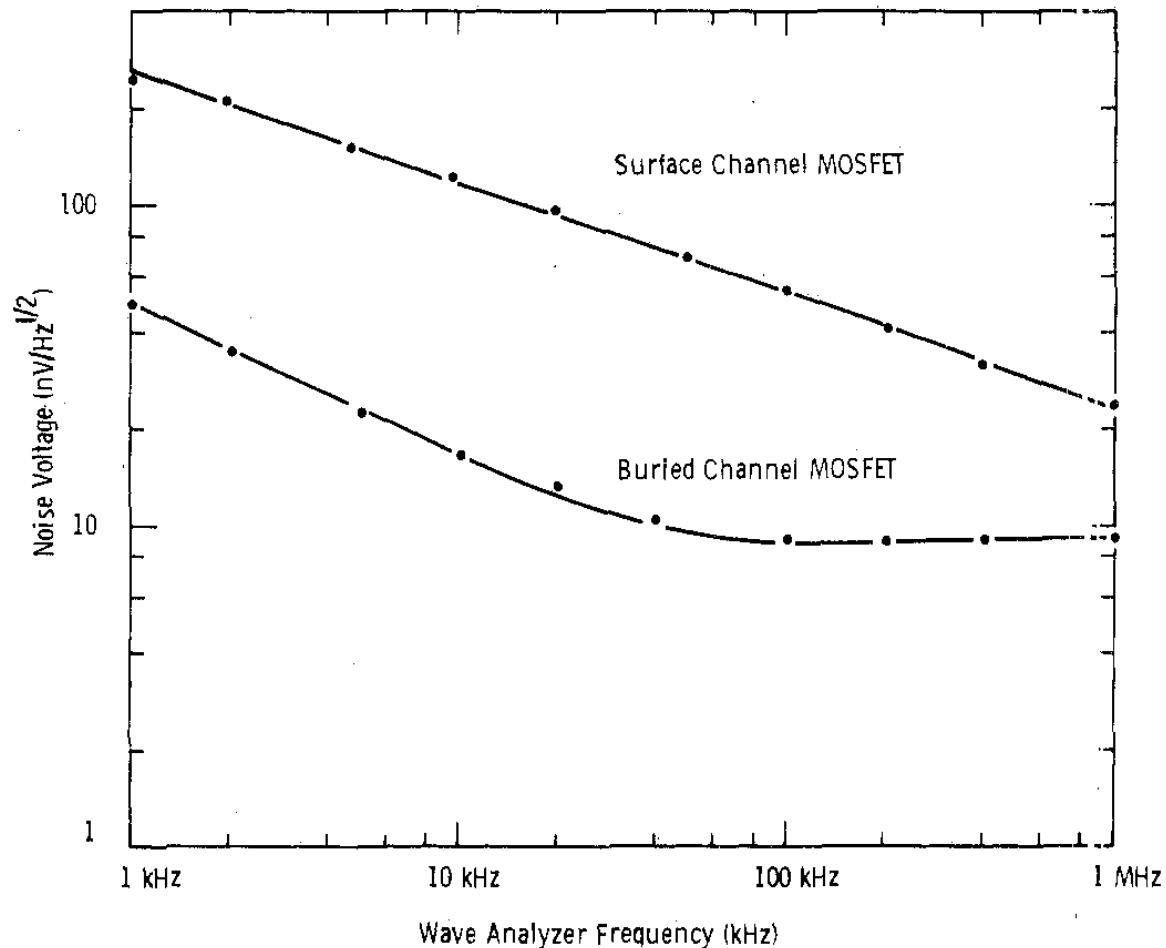
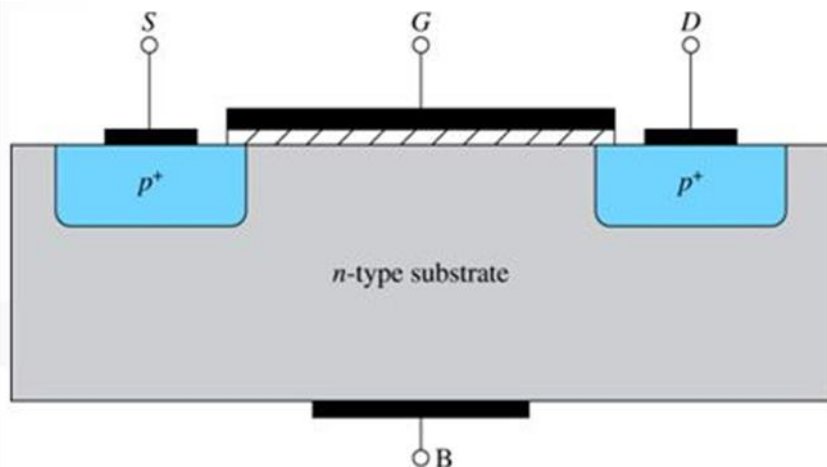
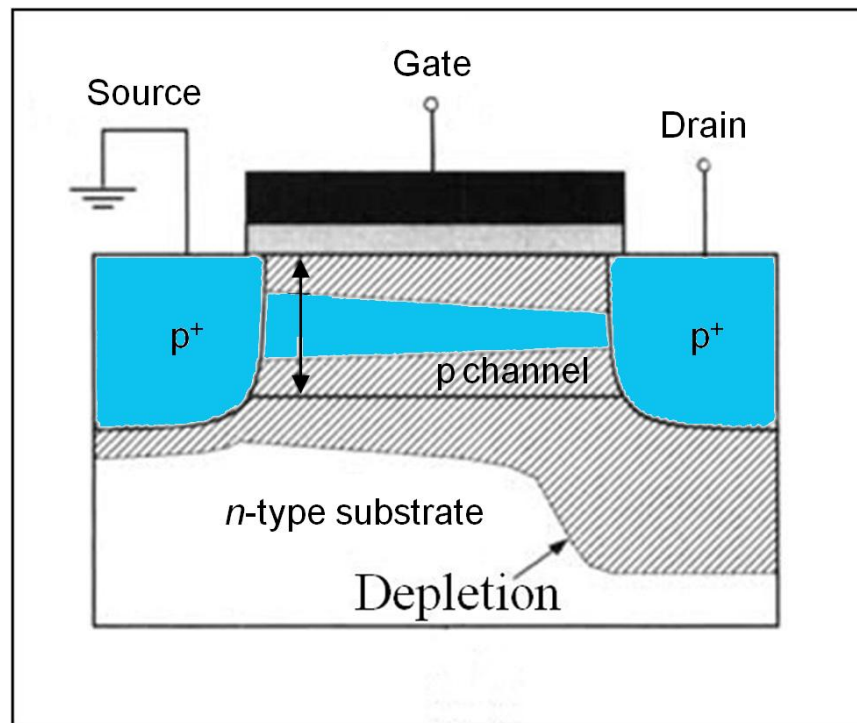


Fig. 4. Comparison of noise voltage for buried and surface channel MOSFET's.

## • Surface versus buried channel MOSFETs

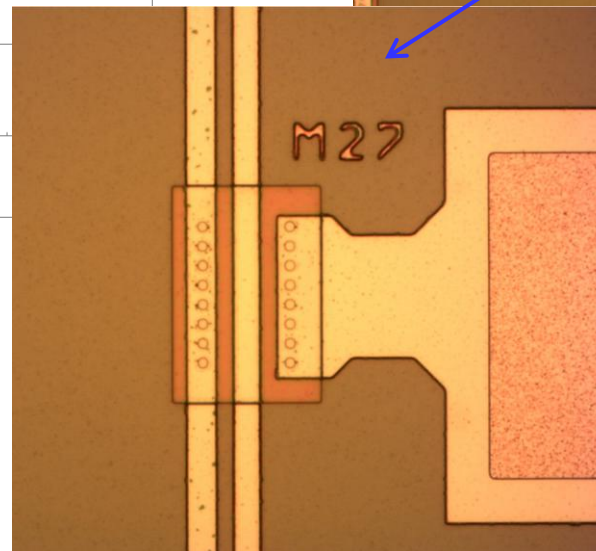
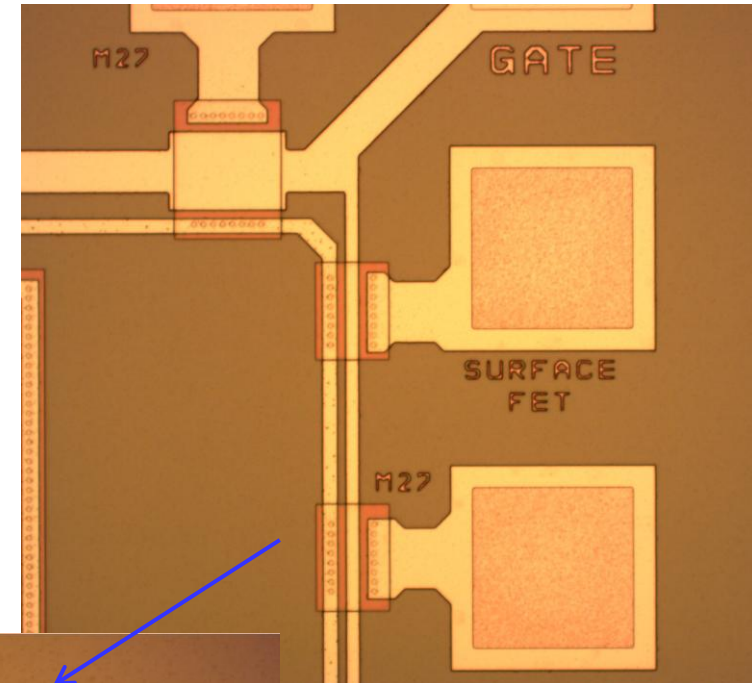
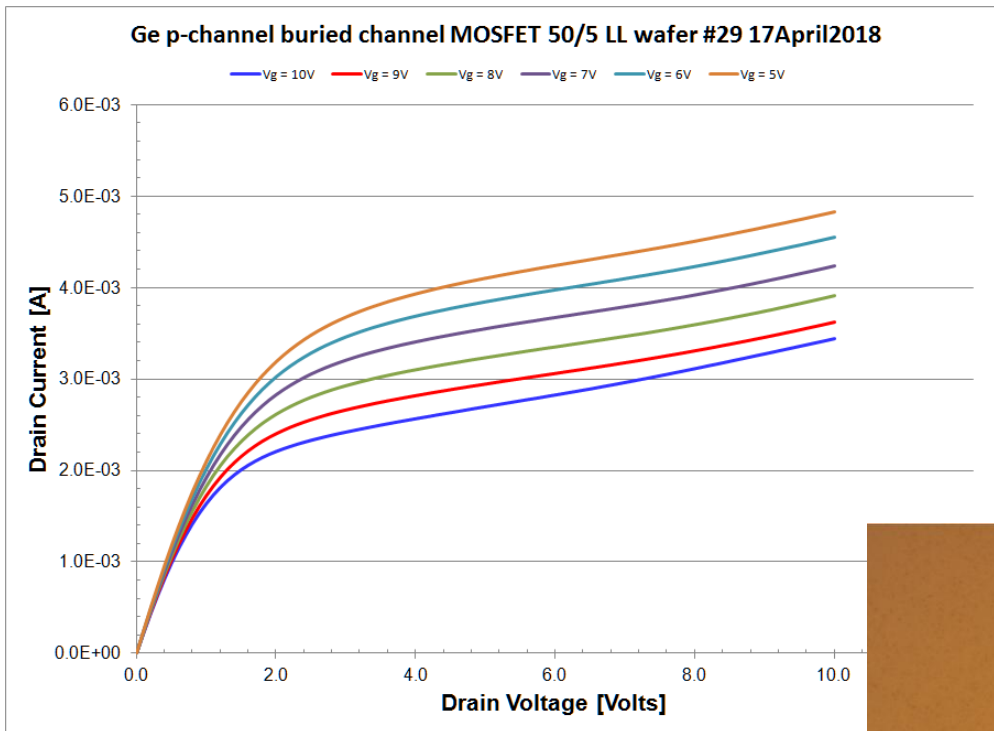


- Surface channel MOSFET
- Conduction in a narrow inversion layer along the surface next to the gate insulator
- Interface-states trap charge and increase the 1/f noise



- Buried channel MOSFET
- Conduction below the surface (blue region)
- Less sensitive to interface states

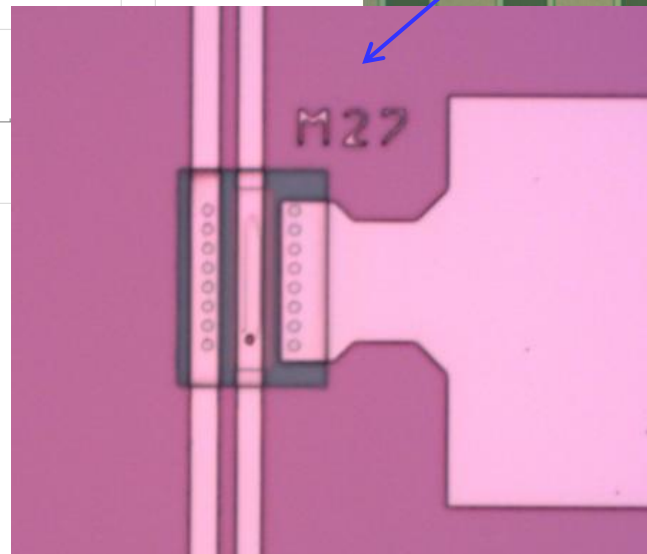
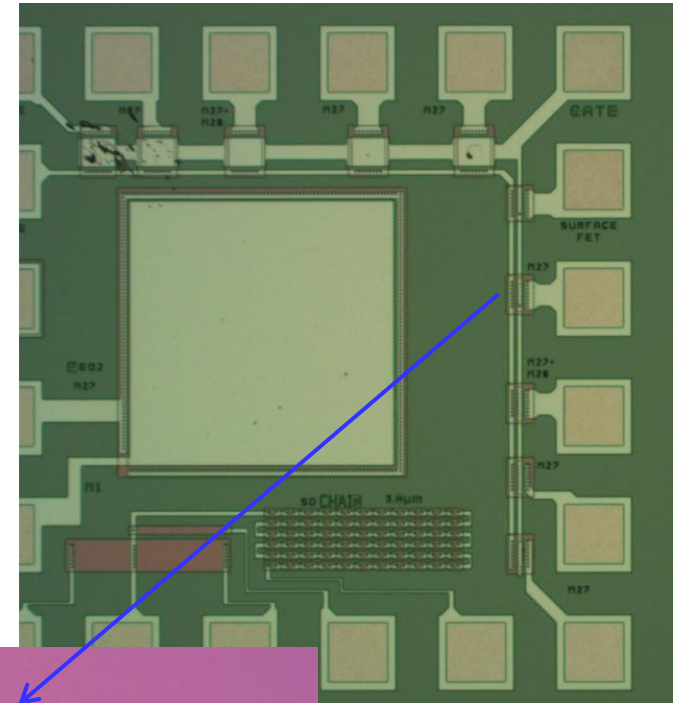
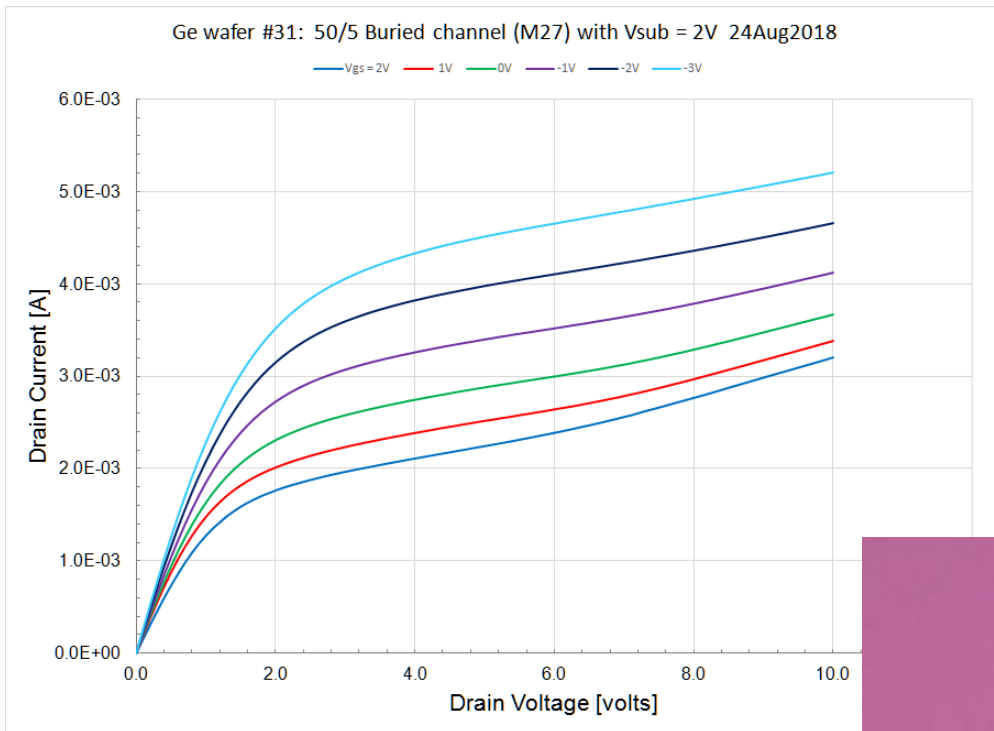
- Germanium buried-channel MOSFET fabricated at the LBNL MicroSystems Lab



PECVD<sup>†</sup> SiO<sub>2</sub> gate dielectric  
Metal-gate transistor

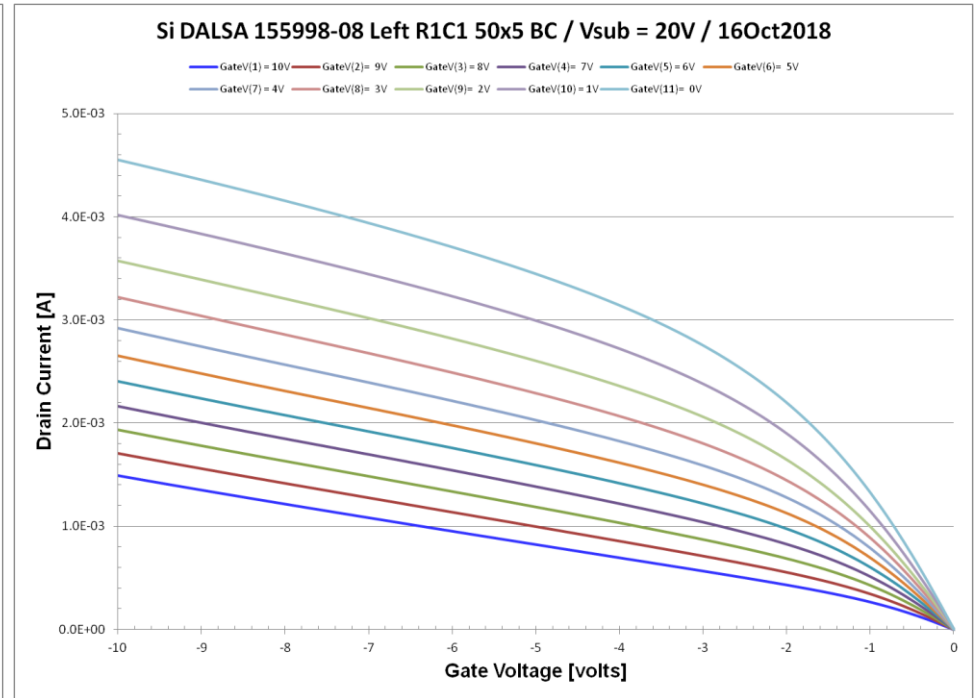
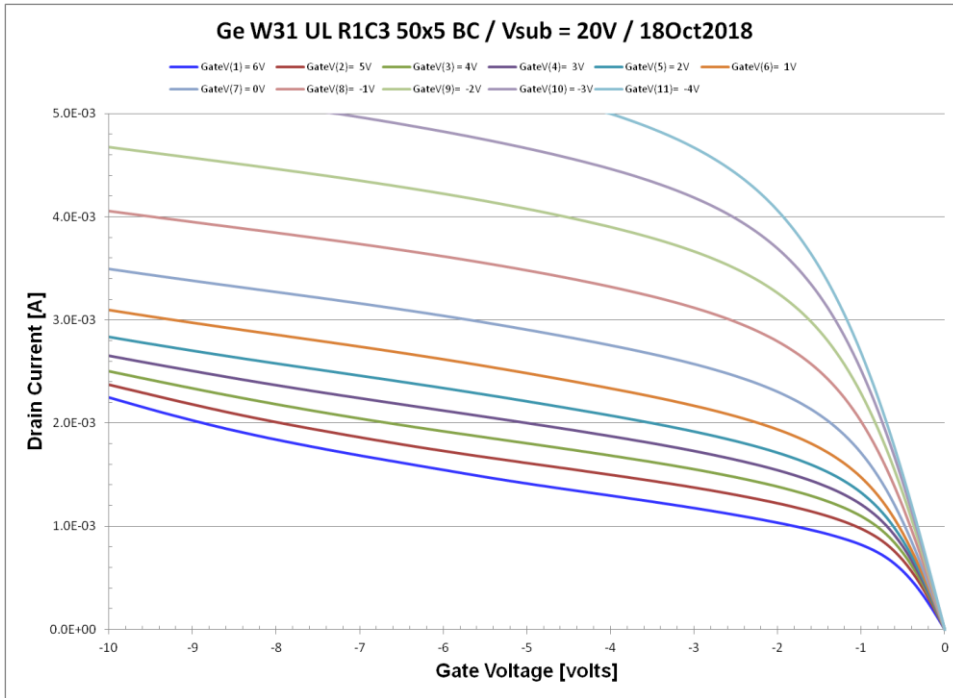
<sup>†</sup> Plasma-enhanced chemical vapor deposition

- Germanium buried-channel MOSFET fabricated at the LBNL MicroSystems Lab



$SiO_2-GeO_2$  gate dielectric  
Metal-gate transistor

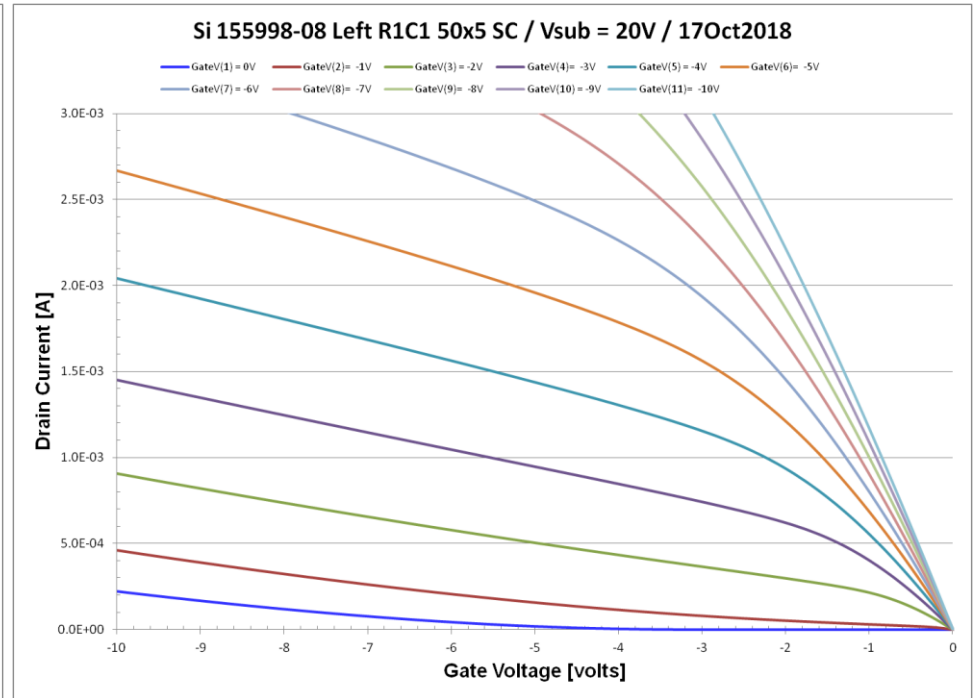
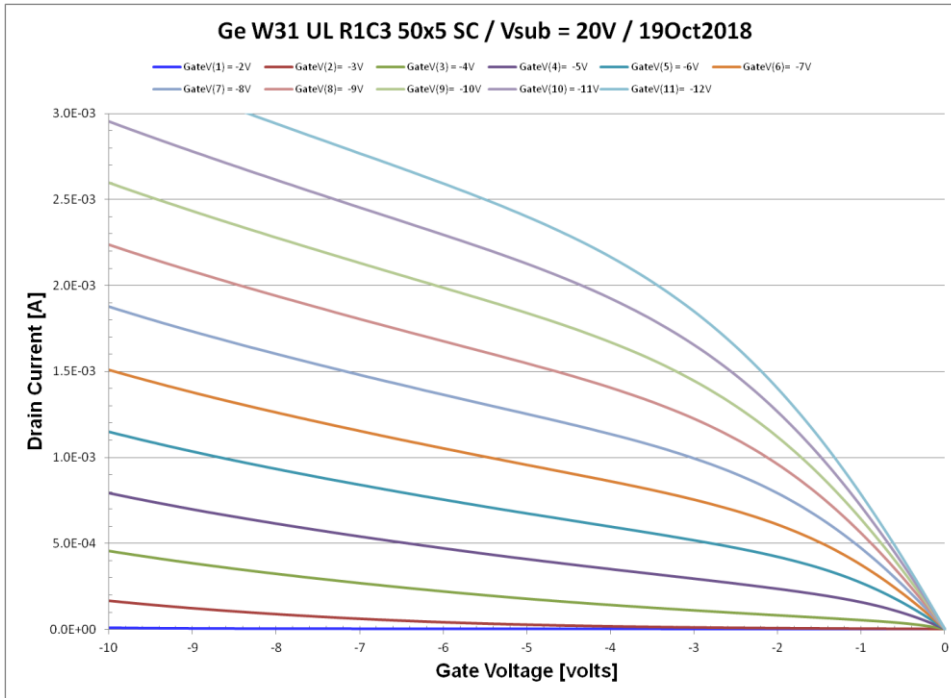




- Ge buried channel MOSFET
- W/L: 50 um / 5 um
- Metal gate

- Si buried channel MOSFET
- W/L: 50 um / 5 um
- Polysilicon gate

Detailed comparisons difficult, but encouraging that the Ge MOSFET has similar performance to the Si device

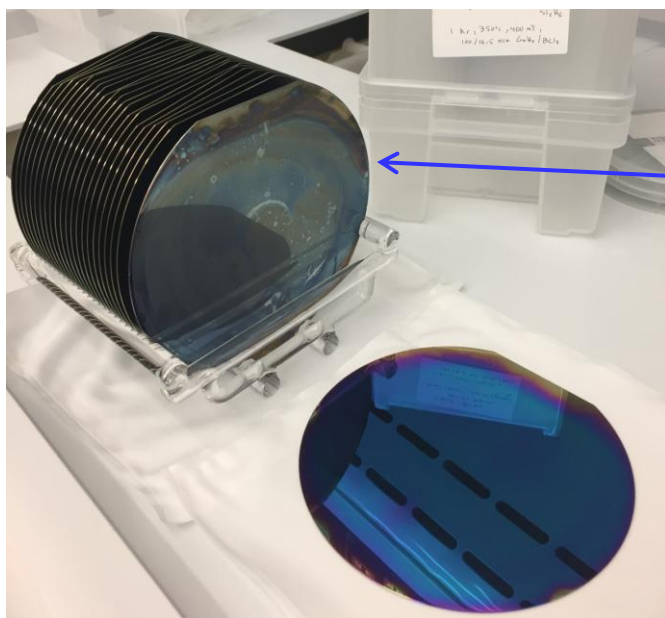


- Ge surface channel MOSFET
- W/L 50 um / 5 um
- Metal gate

- Si surface channel MOSFET
- W/L 50 um / 5 um
- Polysilicon gate

Ge surface channel MOSFET appears to be inferior  
 $\text{GeO}_2/\text{Ge}$  versus  $\text{SiO}_2/\text{Si}$  interface

- Non-ideal effects noted in the first transistor fabrication, the worst shown below
  - 600°C oxidation step on a Ge wafer with no coating on the backside of the wafer
  - Adjacent silicon wafer had blue film deposited that was water soluble (likely  $\text{GeO}_2$ )



Back side of a Ge wafer  
after 1 hour, 600°C in  $\text{O}_2$

Water soluble film deposited on  
adjacent, oxidized silicon wafer

[CONTRIBUTION FROM THE CHEMISTRY DEPARTMENT OF ILLINOIS INSTITUTE OF TECHNOLOGY]

## The Kinetics of the Reaction of Germanium and Oxygen

BY RICHARD B. BERNSTEIN AND DANIEL CUBICCIOTTI

The rate of oxidation of germanium has been measured in the range 575 to 705°. The kinetics do not conform to any of the previously observed rate laws for metal oxidations but rather follow an equation of the form  $Q = Q_{\infty}(1 - e^{-kt})$ , where  $Q$  is the quantity of oxygen consumed by the metal in time  $t$ ;  $Q_{\infty}$  and  $k$  are constants.  $Q_{\infty}$  varies approximately inversely to the oxygen pressure in the range 2 to 40 cm. and the rate constant,  $k$ , is temperature dependent. A mechanism is proposed in which the oxidation rate is controlled by the rate of evaporation of germanium monoxide. This rate of evaporation is in turn governed by the extent to which the surface is covered by impervious germanium dioxide.

Of the two oxides reported for germanium the monoxide is considerably more volatile than the dioxide.<sup>1</sup> This order of volatility may be contrasted with that of the majority of other metals which have volatile oxides, such as tungsten and molybdenum, where the higher oxide is the more volatile. The kinetics of the germanium oxidation have been found to be unusual because of this volatility.

planar spacings of germanium.<sup>3</sup> The patterns of oxidized samples also showed lines corresponding to germanium dioxide.<sup>3</sup> No extra lines were found in any of the patterns.

The brown substance was assumed<sup>4</sup> to be the germanium monoxide reported by Dennis and Hulse.<sup>1</sup> It was obviously more volatile than the white germanium dioxide since it was found in the cold part of the silica tube while the dioxide was found deposited in the hot zone of the tube. Apparently, the germanium monoxide evaporated from the metal surface during the oxidation. Most of it was then oxidized in the tube to the dioxide which deposited on the

After oxidation the sample was coated with a thin blue film; the samples that were most extensively oxidized had a light-colored powdery film in addition. There was a deposit of white powder on the walls of the silica bulb near the sample and often a thin deposit of brown material at the cold end of the tube. When this brown film was heated in air, it seemed to evaporate and oxidize to a cloud of white powder which was unaffected by further heating.

paper, measuring with number 470. The resulting rectangular parallelepiped was used for several runs; between runs it was repolished and weighed. The sample was generally found to have lost weight at the end of a run.

After oxidation the sample was coated with a thin blue film; the samples that were most extensively oxidized had a light-colored powdery film in addition. There was a deposit of white powder on the walls of the silica bulb near the sample and often a thin deposit of brown material at the cold end of the tube. When this brown film was heated in air, it seemed to evaporate and oxidize to a cloud of white powder which was unaffected by further heating.

X-Ray diffraction patterns were obtained from the edges of blocks of metal and oxidized specimens. The patterns of the germanium showed spots corresponding to all the inter-

of the usual metal oxidation.

It is possible to express the oxidation curves accurately by the equation

$$Q = Q_{\infty}(1 - e^{-kt})$$

(3) Am. Soc. Testing Met., "X-Ray Diffraction Patterns," 1942, Second Supplementary Set, 1950.

(4) A sample of this brown material, obtained as a sublimate on heating the metal in 0.1 mm. of oxygen, was found to have the composition  $\text{GeO}_{1.4}$ . The analysis was made by measuring the uptake of oxygen at 1 atm. and 1000°. A sample of germanium subjected to this method of analysis, as a check, took up 98% of the amount of oxygen calculated for the dioxide. Therefore, the brown material had the composition of  $\text{GeO}$ .

(5) For a discussion of the types of oxidation laws see: E. A. Gulbransen, *Trans. Electrochem. Soc.*, **91**, 573 (1947).

(1) L. Dennis and R. Hulse, *THIS JOURNAL*, **52**, 3553 (1930).

(2) D. Cubicciotti, *ibid.*, **72**, 2084, 4138 (1950).

[CONTRIBUTION FROM THE CHEMISTRY DEPARTMENT OF ILLINOIS INSTITUTE OF TECHNOLOGY]

## The Kinetics of the Reaction of Germanium and Oxygen

BY RICHARD B. BERNSTEIN AND DANIEL CUBICCIOTTI

The rate of oxidation of germanium has been measured in the range 575 to 705°. The kinetics do not conform to any of the previously observed rate laws for metal oxidations but rather follow an equation of the form  $Q = Q_{\infty}(1 - e^{-kt})$ , where  $Q$  is the quantity of oxygen consumed by the metal in time  $t$ ;  $Q_{\infty}$  and  $k$  are constants.  $Q_{\infty}$  varies approximately inversely to the oxygen pressure in the range 2 to 40 cm. and the rate constant,  $k$ , is temperature dependent. A mechanism is proposed in which the oxidation rate is controlled by the rate of evaporation of germanium monoxide. This rate of evaporation is in turn governed by the extent to which the surface is covered by impervious germanium dioxide.

Of the two oxides reported for germanium the monoxide is considerably more volatile than the dioxide.<sup>1</sup> This order of volatility may be contrasted with that of the majority of other metals which have volatile oxides, such as tungsten and molybdenum, where the higher oxide is the more volatile. The kinetics of the germanium oxidation have been found to be unusual because of this volatility.

### Experimental

The apparatus was similar to that used previously<sup>2</sup> for metal oxidations. The system was operated at essentially constant pressure and was capable of detecting changes of the order of a few micrograms of oxygen.

planar spacings of germanium.<sup>3</sup> The patterns of oxidized samples also showed lines corresponding to germanium dioxide.<sup>3</sup> No extra lines were found in any of the patterns.

The brown substance was assumed<sup>4</sup> to be the germanium monoxide reported by Dennis and Hulse.<sup>1</sup> It was obviously more volatile than the white germanium dioxide since it was found in the cold part of the silica tube while the dioxide was found deposited in the hot zone of the tube. Apparently, the germanium monoxide evaporated from the metal surface during the oxidation. Most of it was then oxidized in the tube to the dioxide which deposited on the hot walls, while some of the monoxide diffused to the cold walls and deposited there as the brown material.

The fact that the weight losses of the samples were not due to evaporation of germanium itself was determined by evaporation experiments carried out with unoxidized samples in a  $10^{-6}$  mm. vacuum at 800°. In a period of four hours

Apparently, the germanium monoxide evaporated from the metal surface during the oxidation. Most of it was then oxidized in the tube to the dioxide which deposited on the hot walls, while some of the monoxide diffused to the cold walls and deposited there as the brown material.

pany, was fused *in vacuo* and then polished with emery paper, finishing with number 4/0. The resulting rectangular parallelepiped was used for several runs; between runs it was repolished and weighed. The sample was generally found to have lost weight at the end of a run.

After oxidation the sample was coated with a thin blue film; the samples that were most extensively oxidized had a light-colored powdery film in addition. There was a deposit of white powder on the walls of the silica bulb near the sample and often a thin deposit of brown material at the cold end of the tube. When this brown film was heated in air, it seemed to evaporate and oxidize to a cloud of white powder which was unaffected by further heating.

X-Ray diffraction patterns were obtained from the edges of blocks of metal and oxidized specimens. The patterns of the germanium showed spots corresponding to all the inter-

pressure, in contrast to the pressure independence of the usual metal oxidation.

It is possible to express the oxidation curves accurately by the equation

$$Q = Q_{\infty}(1 - e^{-kt})$$

(3) Am. Soc. Testing Met., "X-Ray Diffraction Patterns," 1942, Second Supplementary Set, 1950.

(4) A sample of this brown material, obtained as a sublimate on heating the metal in 0.1 mm. of oxygen, was found to have the composition  $\text{GeO}_{1.4}$ . The analysis was made by measuring the uptake of oxygen at 1 atm. and 1000°. A sample of germanium subjected to this method of analysis, as a check, took up 96% of the amount of oxygen calculated for the dioxide. Therefore, the brown material had the composition of  $\text{GeO}$ .

(5) For a discussion of the types of oxidation laws see: E. A. Gulbransen, *Trans. Electrochem. Soc.*, **91**, 573 (1947).

(1) L. Dennis and R. Hulse, *THIS JOURNAL*, **52**, 3553 (1930).

(2) D. Cubicciotti, *ibid.*, **72**, 2084, 4138 (1950).



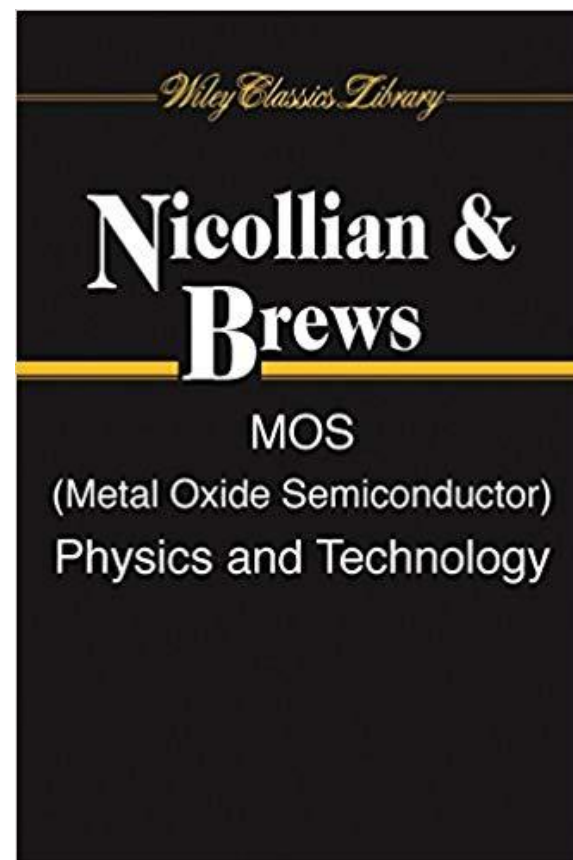
## LBNL Ge R&D (LDRD)

- We now coat the backsides of the Ge wafers with  $\text{SiO}_2$  to inhibit the oxidation and the consequent  $\text{GeO}$  /  $\text{GeO}_2$  issues
- We next fabricated capacitor-only wafers to see if the  $\text{Ge-GeO}_2$  interface could be improved via process changes and address some of the issues seen in the first attempt
  - Simple 2 mask process
  - No ion implantation steps



# LBNL Ge R&D (LDRD)

- MOS capacitors used to study the quality of the gate insulator and the semiconductor-insulator interface
- C-V curves yield much information about the quality of the insulator
- After much R&D in the 1970's, the Si-SiO<sub>2</sub> interface typically has defect levels in the low 10<sup>10</sup> cm<sup>-2</sup>, or about 1 defect per every 10<sup>5</sup> Si atoms
  - Ge-GeO<sub>2</sub> interface is at best 10x worse



- For  $\text{SiO}_2$  the two major advances (1970's) were
  - “Deal triangle”
    - Address fixed oxide charge
  - Post metallization anneal in  $\text{H}_2$ 
    - Minimize interface states
    - $\text{H}_2$  PMA in Ge not effective
  - Implemented on CDF strip detectors in late 1980's

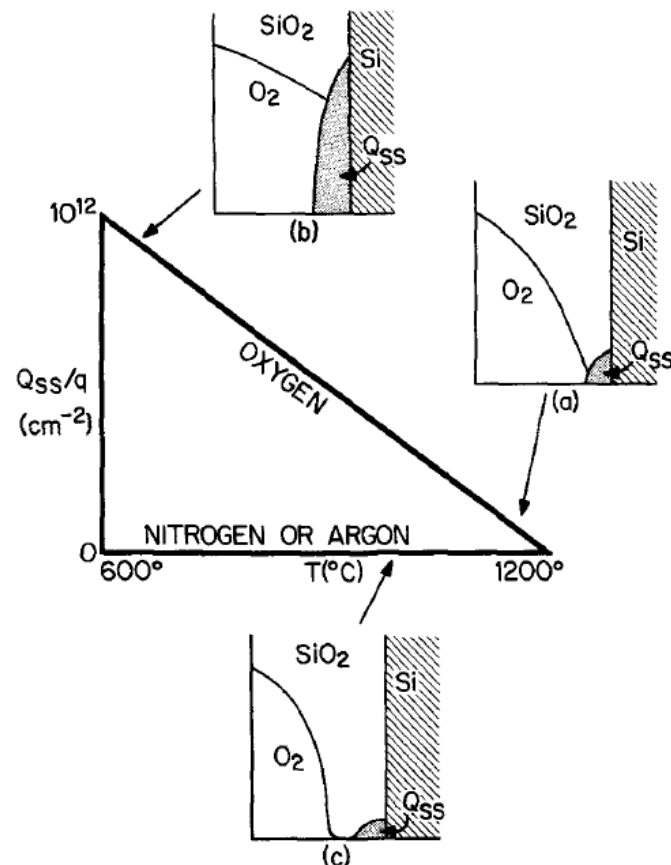


Fig. 6. The dependence of  $Q_{ss}$  on final oxidation temperature and ambient as represented by the  $Q_{ss}$ -oxygen triangle. Data are for (111) oriented silicon. Also shown are sketches of thermal oxide cross section indicating proposed relationship of  $Q_{ss}$  to oxidation conditions.



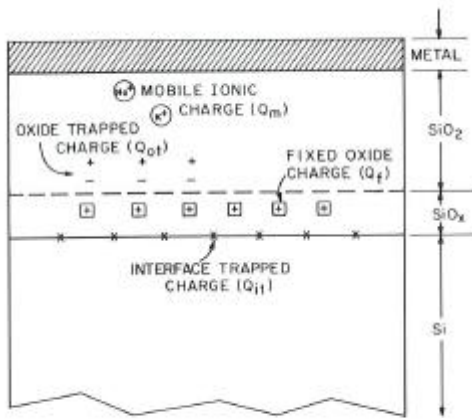
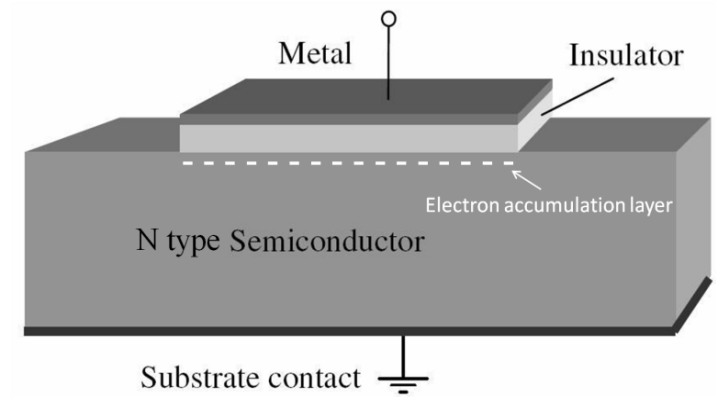


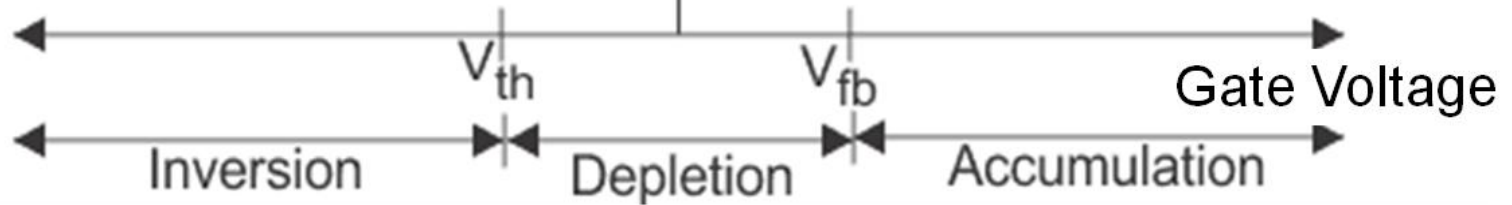
Fig. 15 Terminology for charges associated with thermally oxidized silicon. (After Deal, Ref. 19.)



## Capacitance

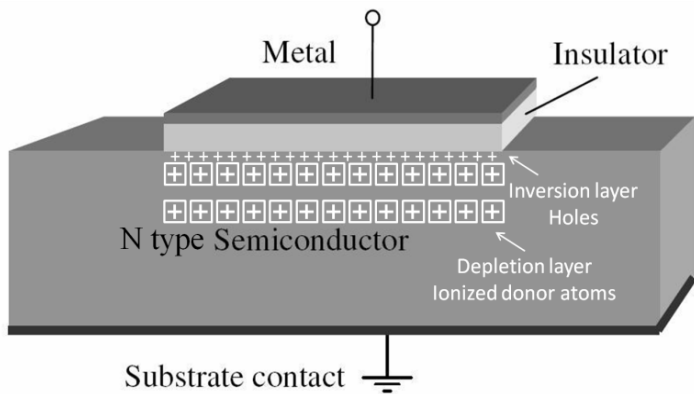
Low frequency

High frequency



$$C_{oxide} = \frac{\epsilon_{oxide} \epsilon_0 Area}{t_{oxide}}$$





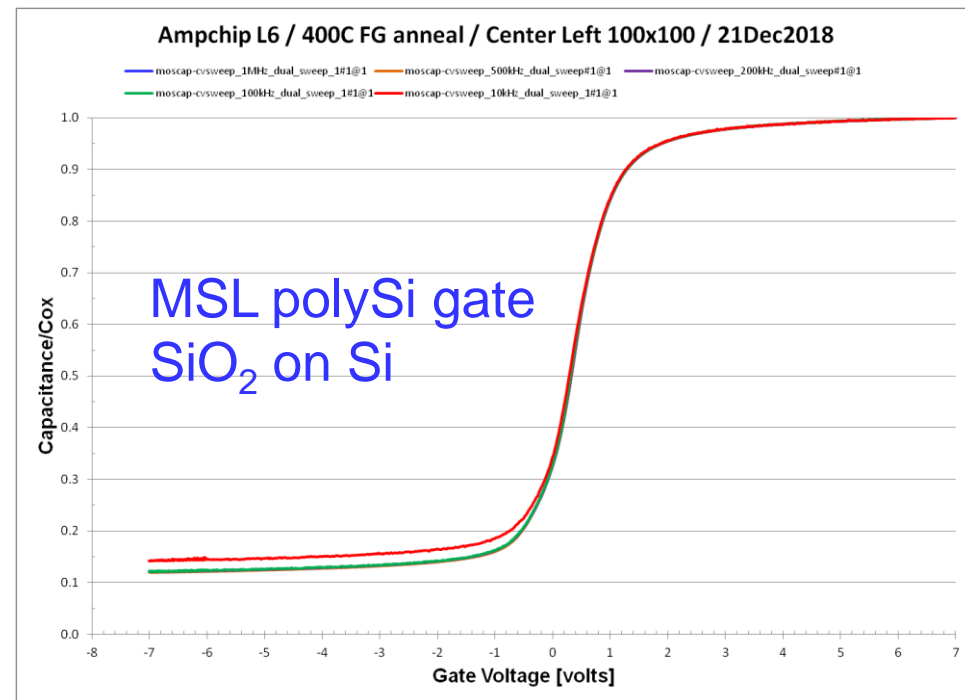
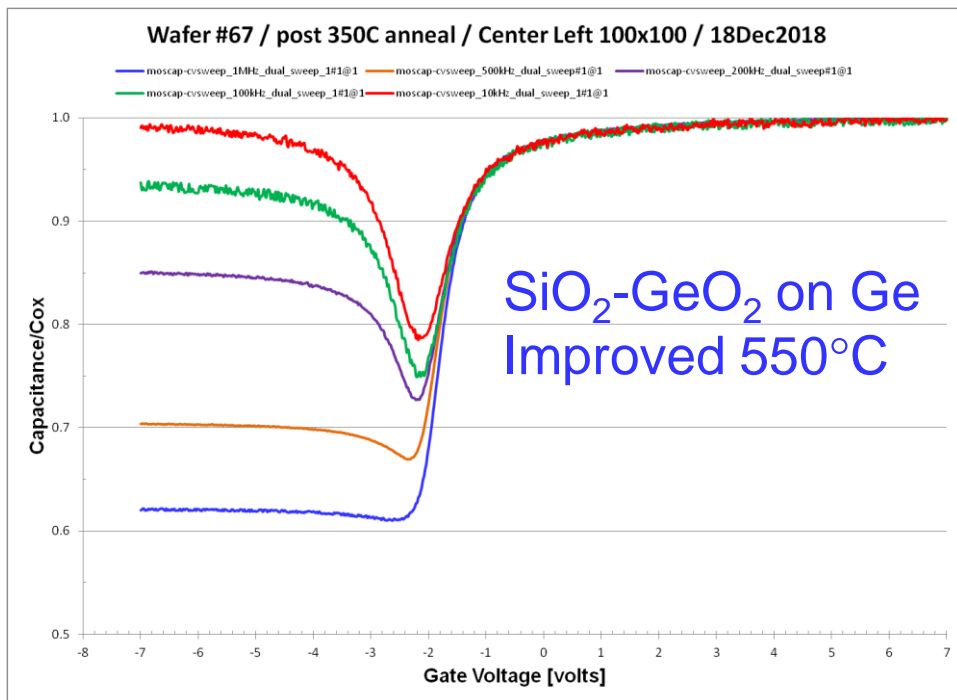
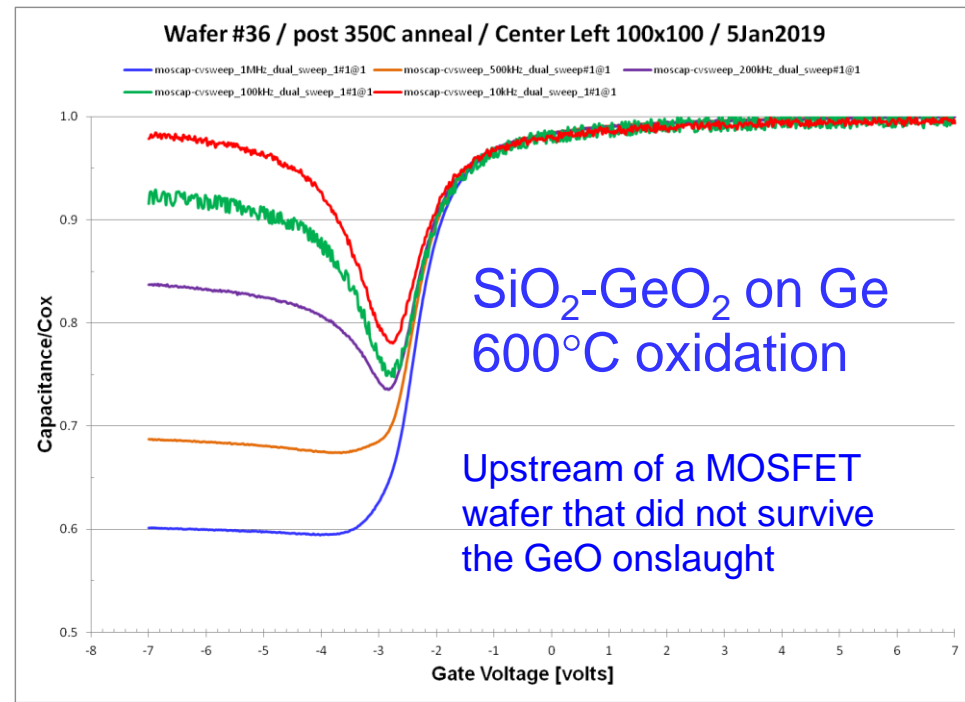
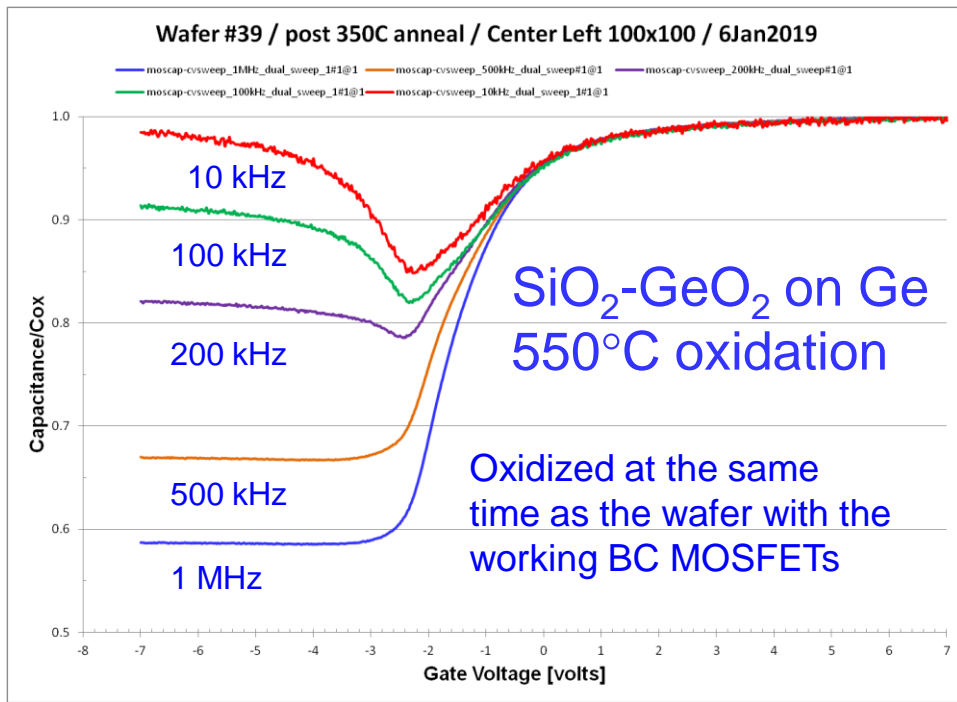
## Capacitance

Low frequency

High frequency

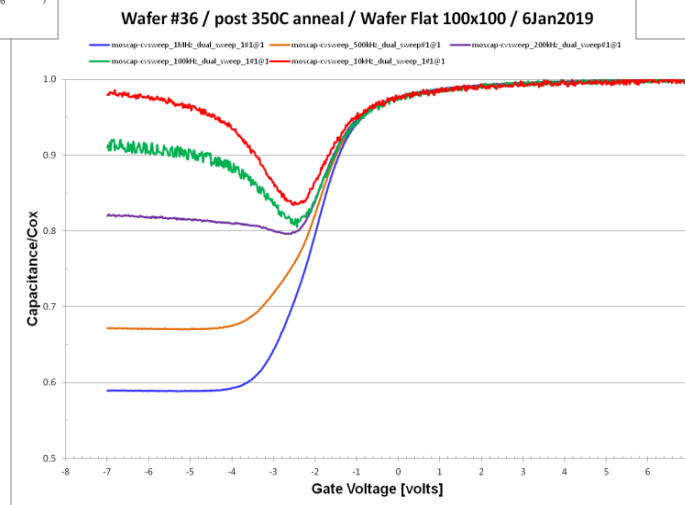
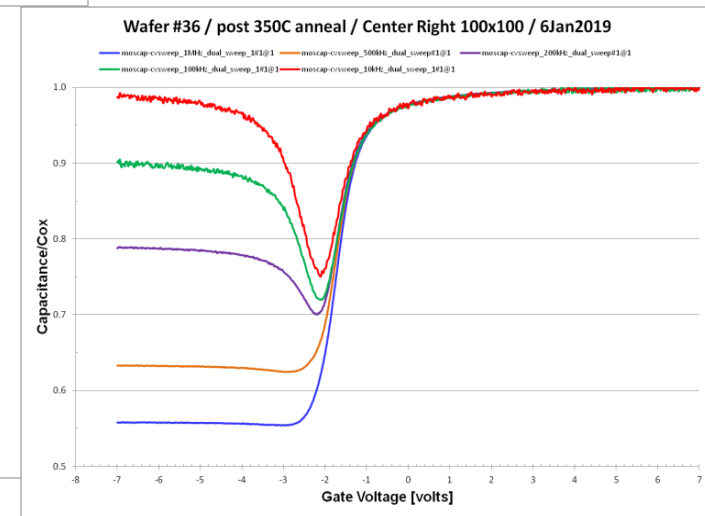
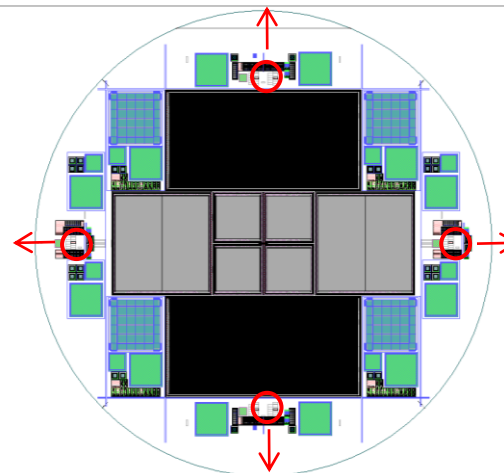
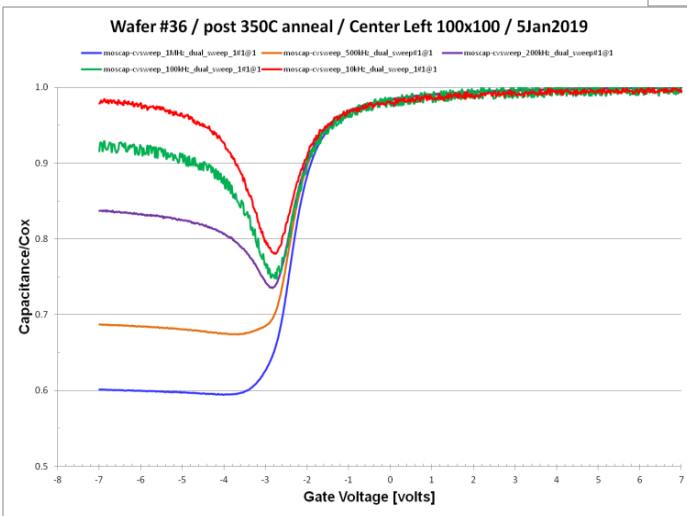
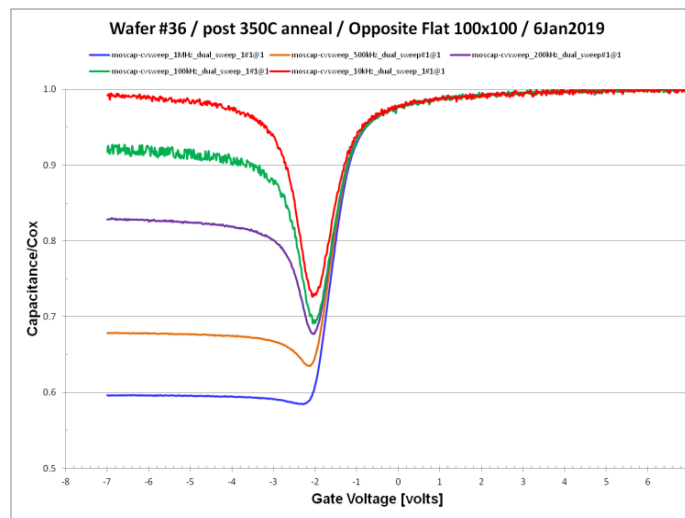
$$\frac{1}{C_{HF}(V)} = \frac{1}{C_{oxide}} + \frac{1}{C_{depletion\_max}}$$





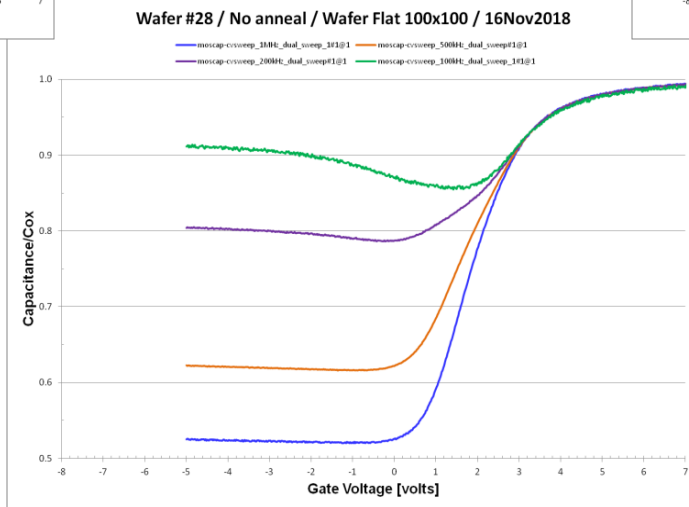
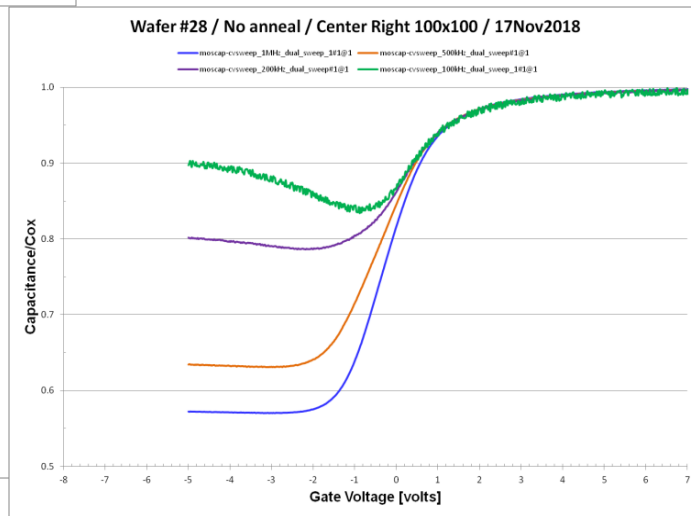
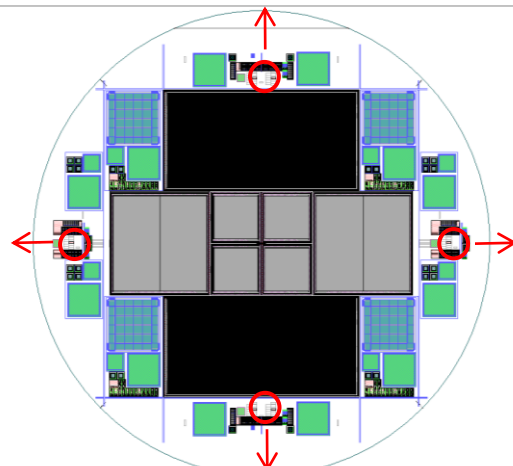
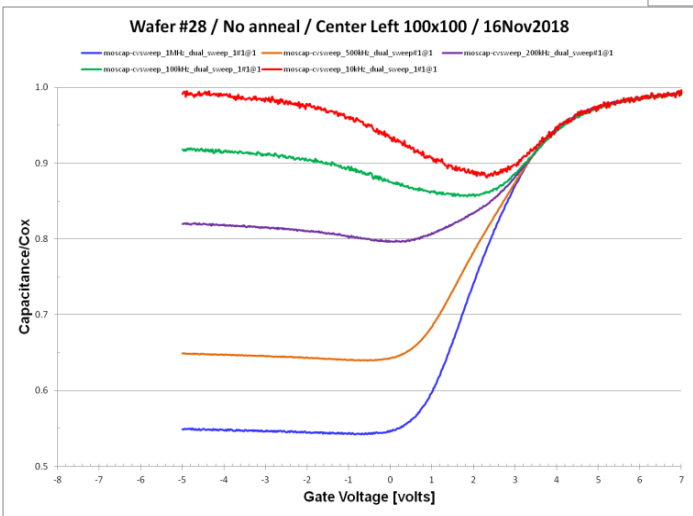
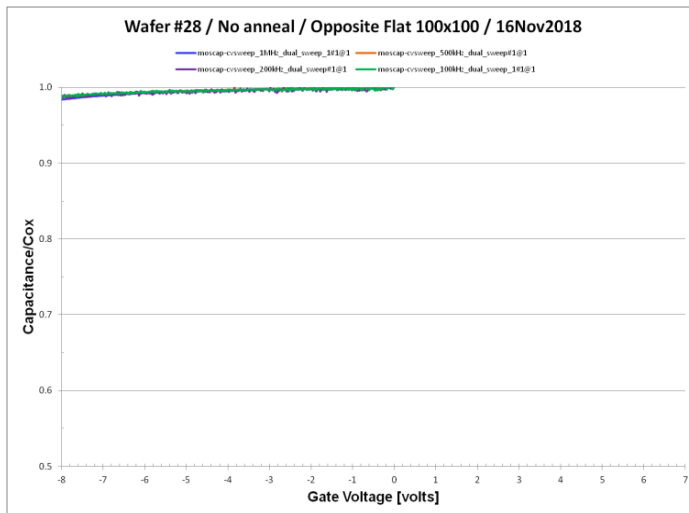
Best so far

SiO<sub>2</sub>-GeO<sub>2</sub> on Ge  
600°C oxidation

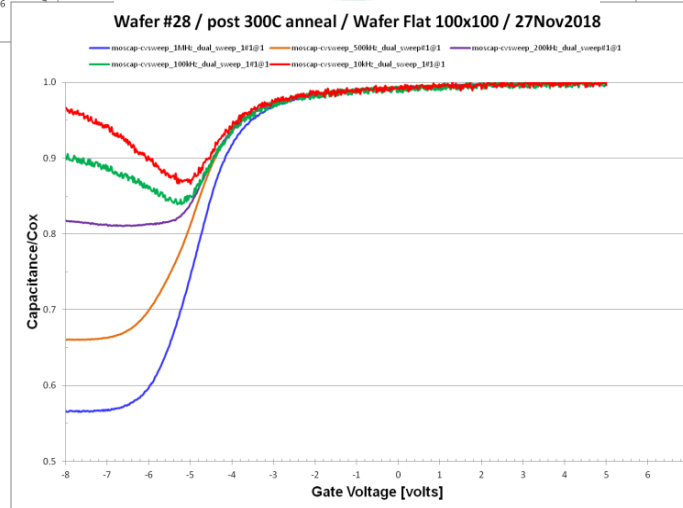
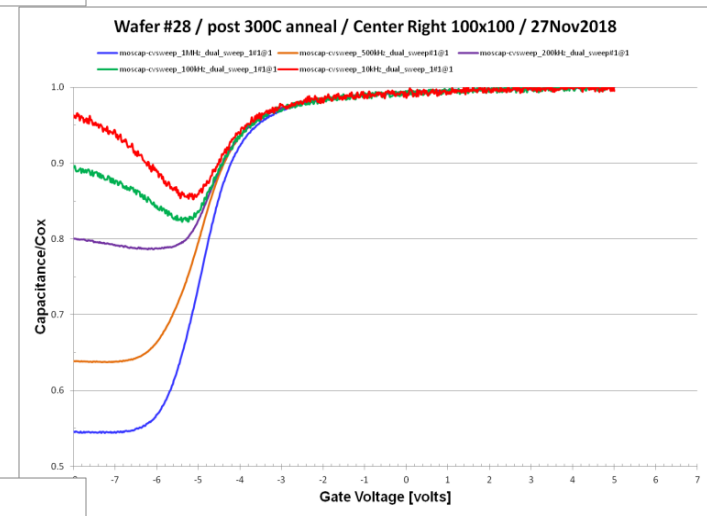
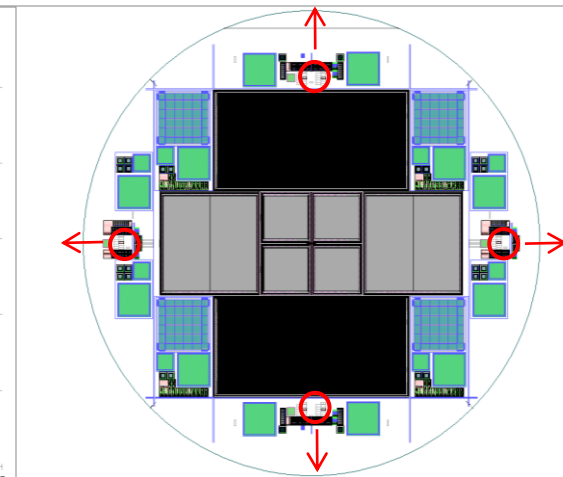
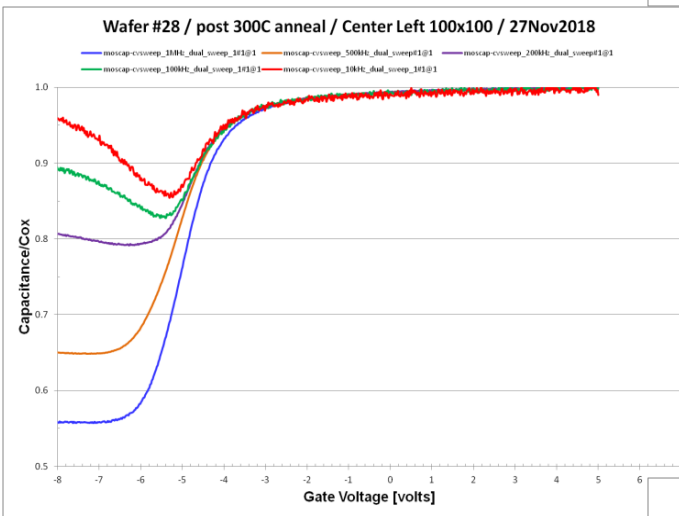
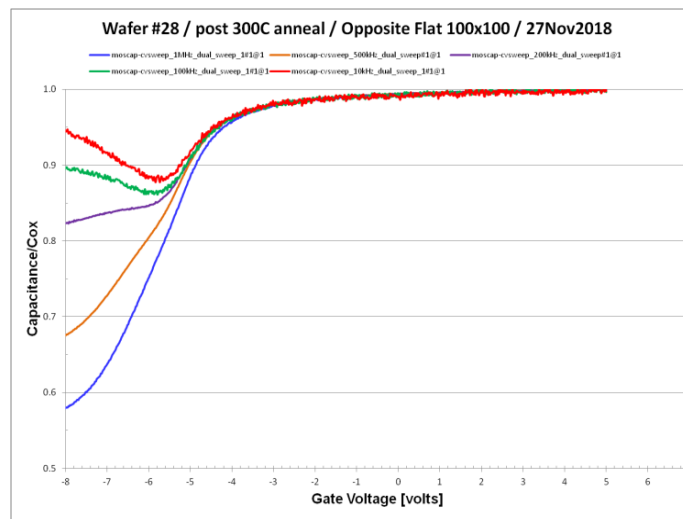


# Post-metallization anneal study

550°C oxidation  
No PMA anneal

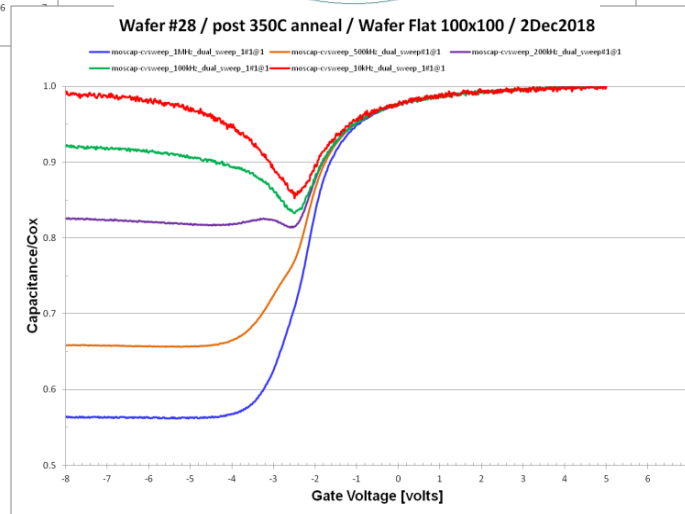
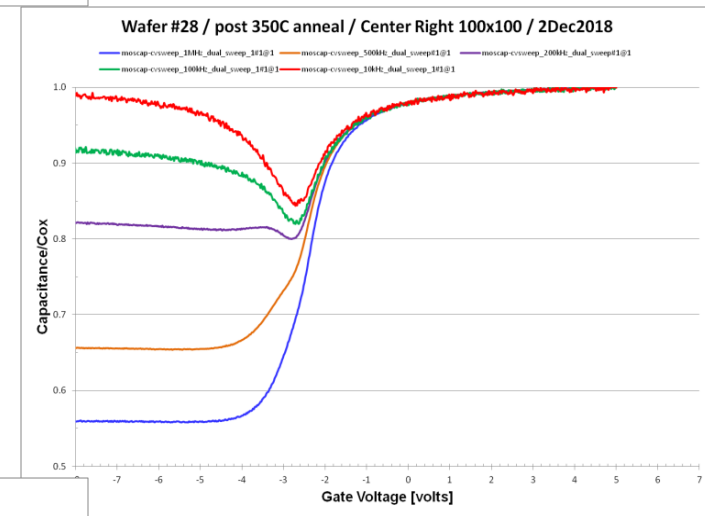
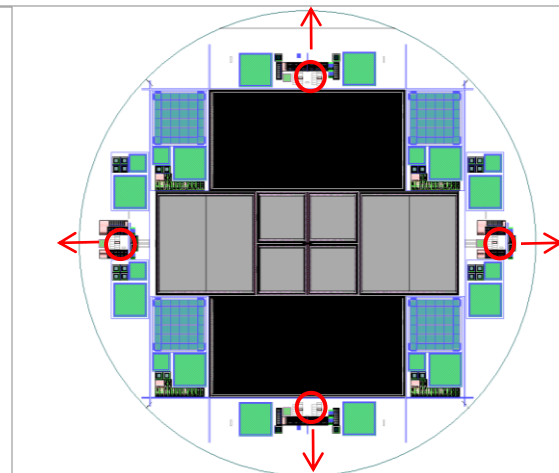
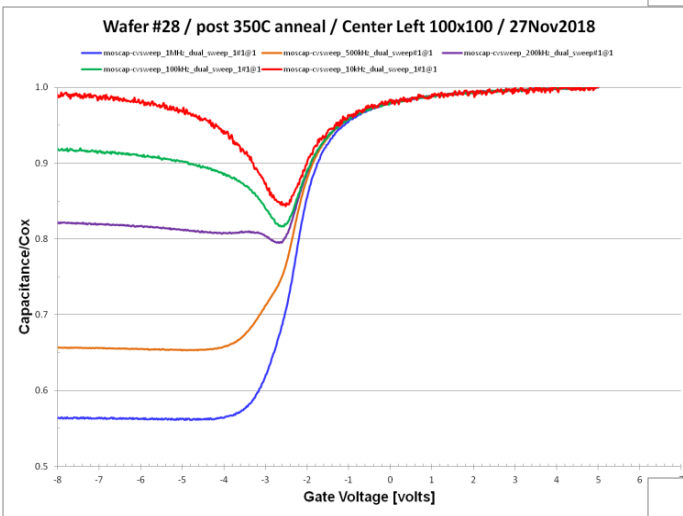
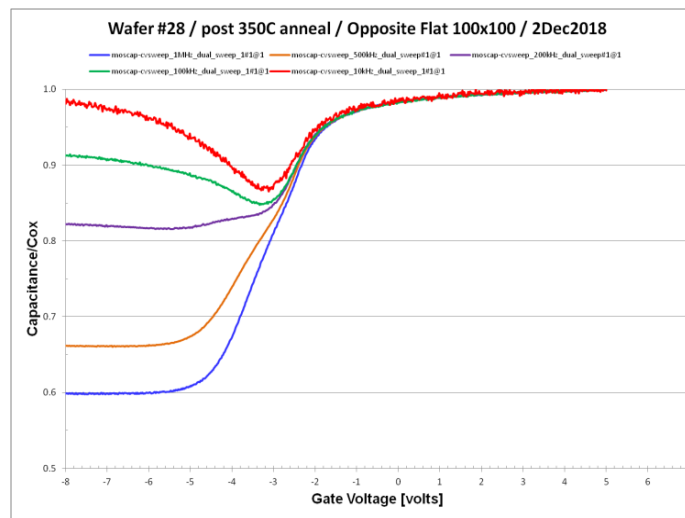


Same wafer  
45 min 300°C



Same wafer

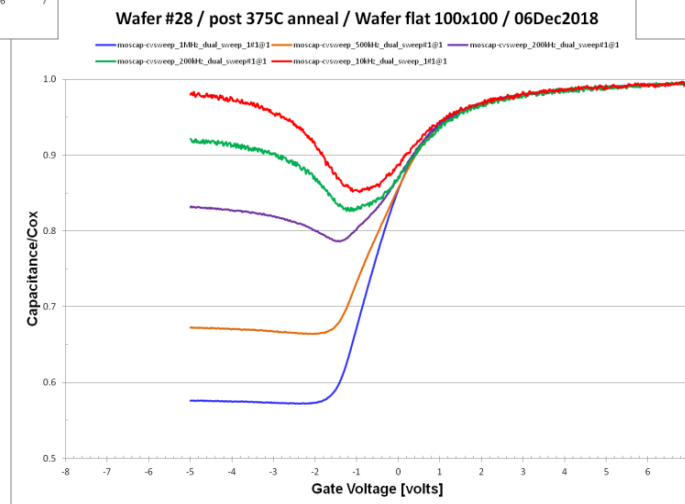
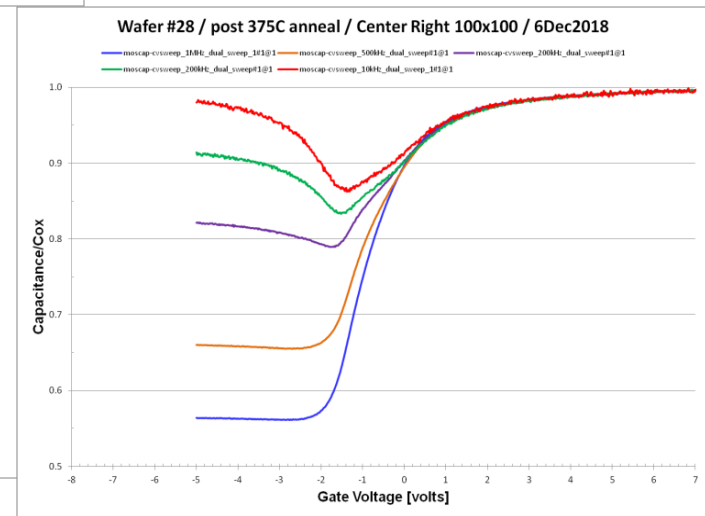
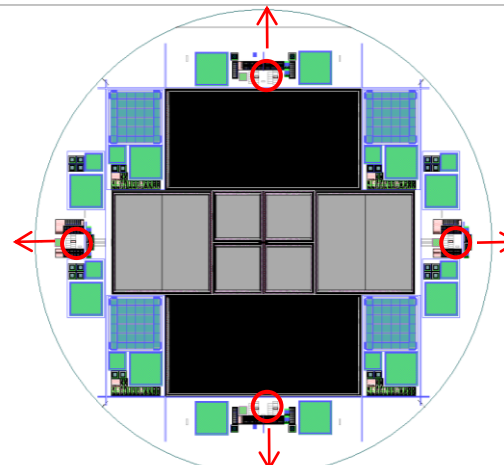
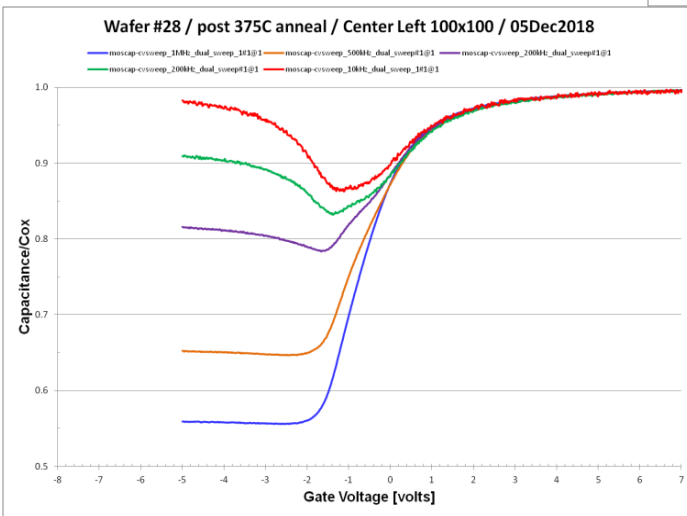
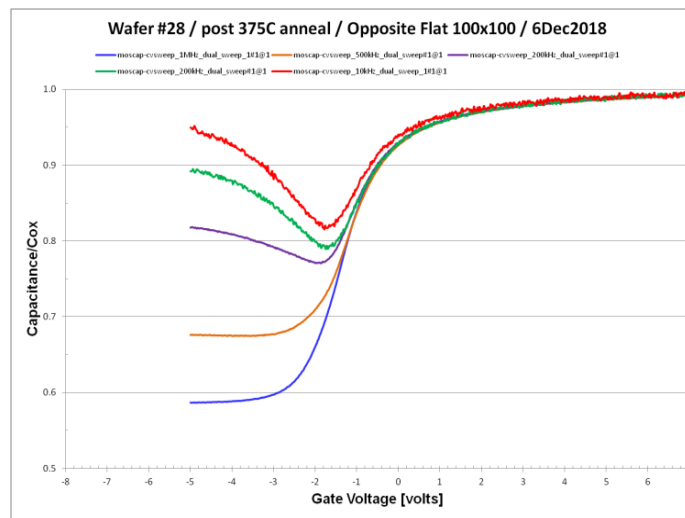
1 hr 350°C

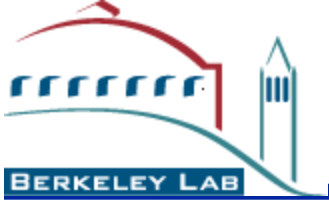




Same wafer

1 hr 375°C





# LBNL Ge R&D (LDRD)

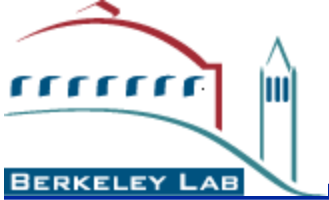
- Three remaining topics
  - High purity Ge wafer production via SBIR
  - Brief overview of work at the UC-Berkeley Marvell Nanofabrication Laboratory
  - Lincoln Labs Ge CCD effort

—The table of material properties shown earlier listed millisecond minority carrier lifetimes

Properties	Si	Ge
Energy gap (eV)	1.12	0.67
Intrinsic carrier concentration (cm <sup>-3</sup> )	1.45 × 10 <sup>10</sup>	2.4 × 10 <sup>13</sup>
Minority carrier lifetime (s)	<del>25</del> × 10 <sup>-3</sup>	10 <sup>-3</sup>

$$J_{leakage} \propto \frac{n_i}{\tau_g} \propto \frac{\exp(-E_g/2kT)}{\tau_g}$$

- Only valid for detector-grade materials
- High resistivity silicon (FD CCDs), HPGe



# LBNL Ge R&D (LDRD)

- Concern that we only have one viable Ge supplier with 10's  $\mu$ sec lifetimes
- Explore the possibility of producing 150 mm wafers from HPGe
  - Analogous to the high-resistivity Si effort
- CCD parameters like dark current and charge transfer efficiency depend critically on lifetime via the presence of harmful impurities
  - » *Deathnium* (W. Shockley)

- From William Shockley's 1956 NP lecture

Holes, electrons, donors and acceptors represent four of the five classes of imperfections that must be considered in semiconductor crystals in order to understand semiconductor effects. The fifth imperfection has been given the name *deathnium*. The chemical analogue of deathnium is a catalyst. In the

**Holes, electrons, donors and acceptors represent four of the five classes of imperfections that must be considered in semiconductor crystals in order to understand semiconductor effects. The fifth imperfection has been given the name *deathnium*.**

this recombination process. The symbols for the five imperfections are shown in Table I.

Table I.

1.  $-$  (excess) electron
2.  $+$  hole
3. deathnium
4.  $\oplus$  donor
5.  $\ominus$  acceptor

- From William Shockley's 1956 NP lecture

Actually, there are several forms of deathnium. For example, if electrons

**Actually, there are several forms of *deathnium*.**

due University, it is known that such bombardment produces disorder of the germanium atoms<sup>3</sup>. A high-energy electron can eject a germanium atom

**... found that copper and nickel chemical impurities in the germanium produce marked reductions in the lifetime.**

It has also been found that copper and nickel chemical impurities in the germanium produce marked reductions in lifetime<sup>4</sup>.

The way in which deathnium catalyzes the recombination process is in-

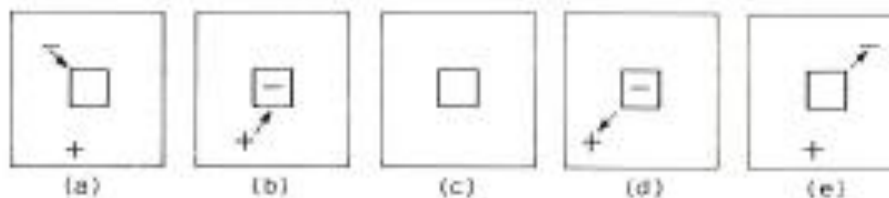
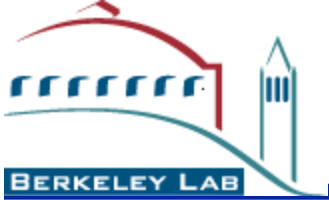


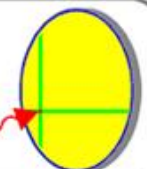
Fig. 1. A recombination center (deathnium) captures alternately an electron and a hole and thus catalyzes their recombination, as shown in parts (a), (b), and (c). The thermally activated generation process is shown in (d) and (e).



# High-purity Ge

- Impressive history at LBNL of HPGe work
  - The late Eugene Haller, R. Pehl, W. Hansen, J. Beeman, Paul Luke of “Luke phonons”, M. Amman, graduate students, e.g. Nick Palaio, apologies for omissions
- With assistance from Maurice Garcia-Sciveres and Helmut Marsiske of the DOE, we placed an SBIR call for HPGe wafer production
- We targeted the company PHDS Co. given that they had received previous SBIRs and were capable of producing 150 mm diameter crystals

PHDs  
Co.



## Growth of large diameter high-purity germanium crystals for Nuclear Physics research

Principal Investigator: Richard Pehl, Ph.D.

Presented by Ethan Hull, Ph.D.

DE-SC0004256

Phase II: 8/15/11-8/14/13

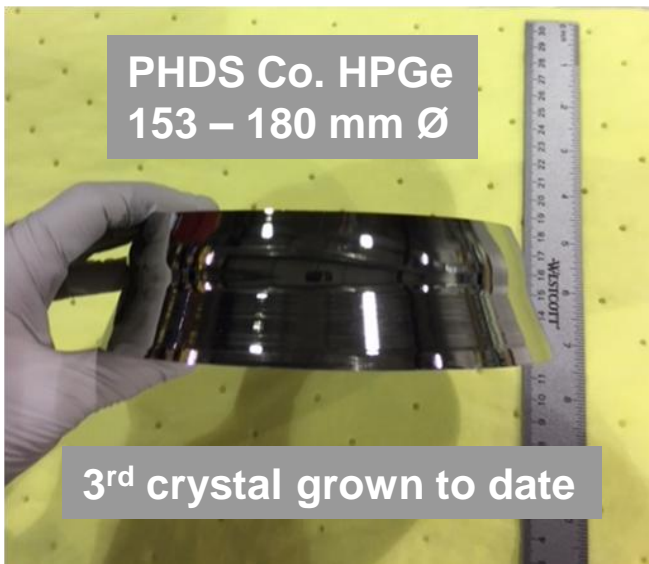
Extremely large diameter (150-200 mm) high-purity germanium crystals are being developed for large diameter Nuclear Physics planar detectors. A high-purity germanium crystal puller has been demonstrated to grow crystals having sufficient purity and charge-collection properties to produce detector-quality germanium. The puller has the capacity to grow very large diameter (~ 200 mm) germanium crystals. The diameter of the germanium crystals and purity levels are being iteratively improved. The results are being constantly monitored through test detector fabrication and gamma-ray spectroscopy measurements.

Collaboration with Kim Lister at UMass Lowell

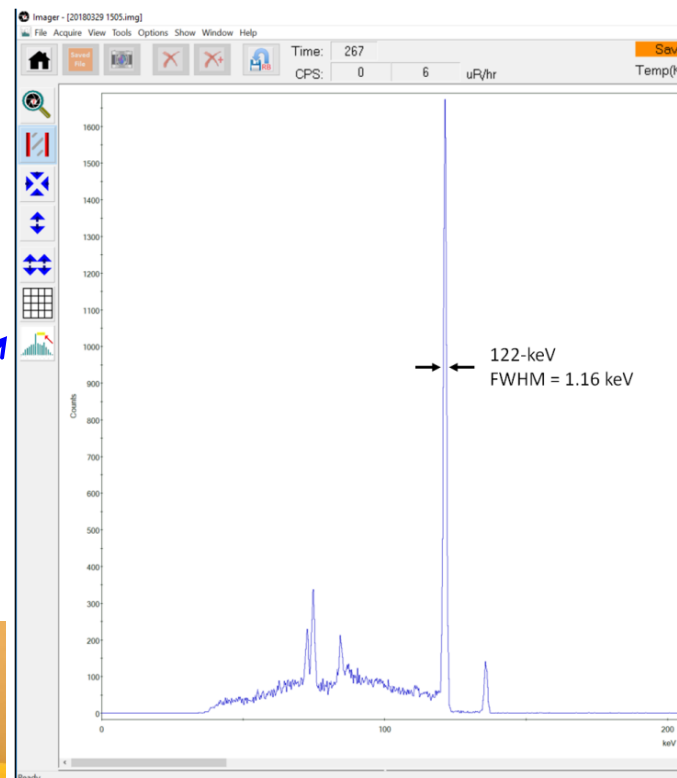
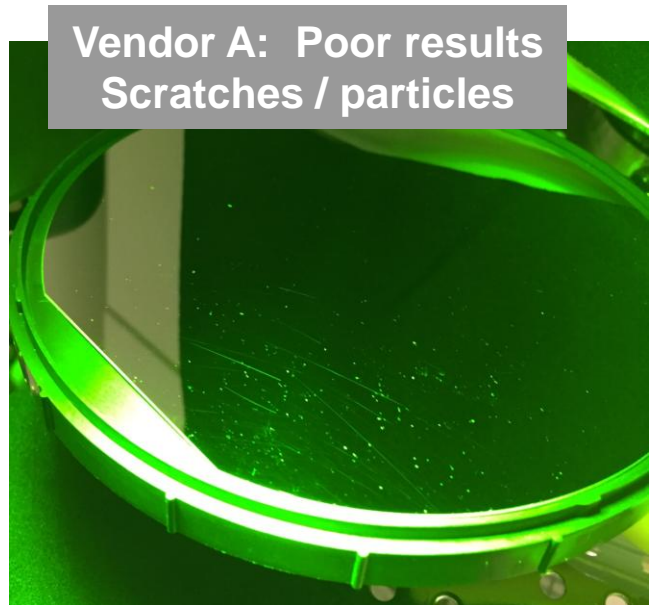
- Material Processing and Crystal Growth at PHDs Co.
- Crystal Measurements and Properties
  - Large diameter challenges
  - Impurity concentration and doping
  - Charge collection
- Products – Nuclear Physics is the basis



- High purity Ge wafer production (SBIR Phase I)

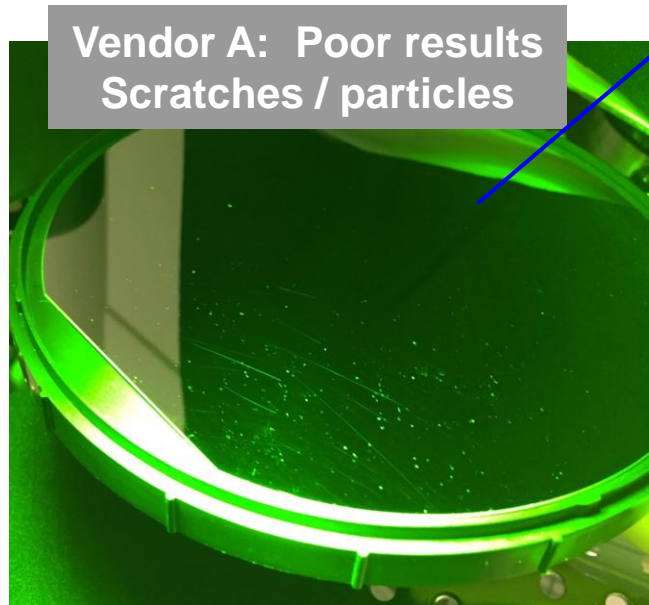
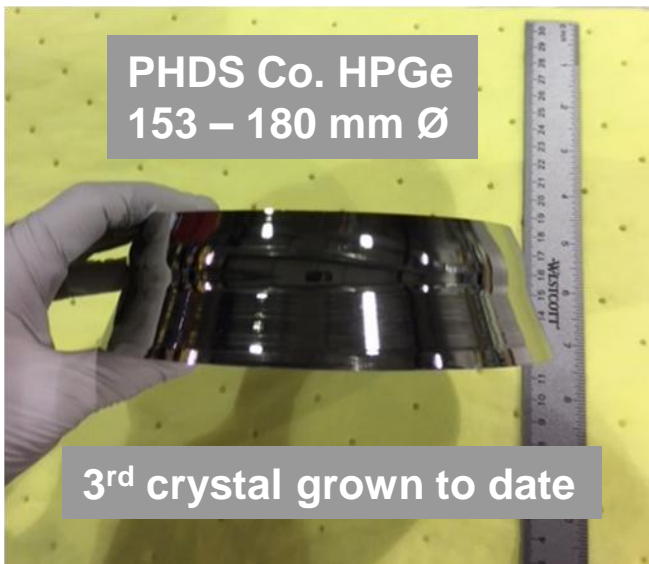


Umicore slicing  
and polishing  
yielded 41 wafers  
(48 mm thick)



$\gamma$ -ray spectra from a  
scrap piece of the Ge  
crystal processed at  
Umicore  
(courtesy PHDS Co.)

- High purity Ge wafer production (SBIR Phase I)



## SUMMARY

### CRYSTAL #1

BULK LIFETIME	41.6 $\mu$ s
SRV	153 cm/s.

### CRYSTAL #3

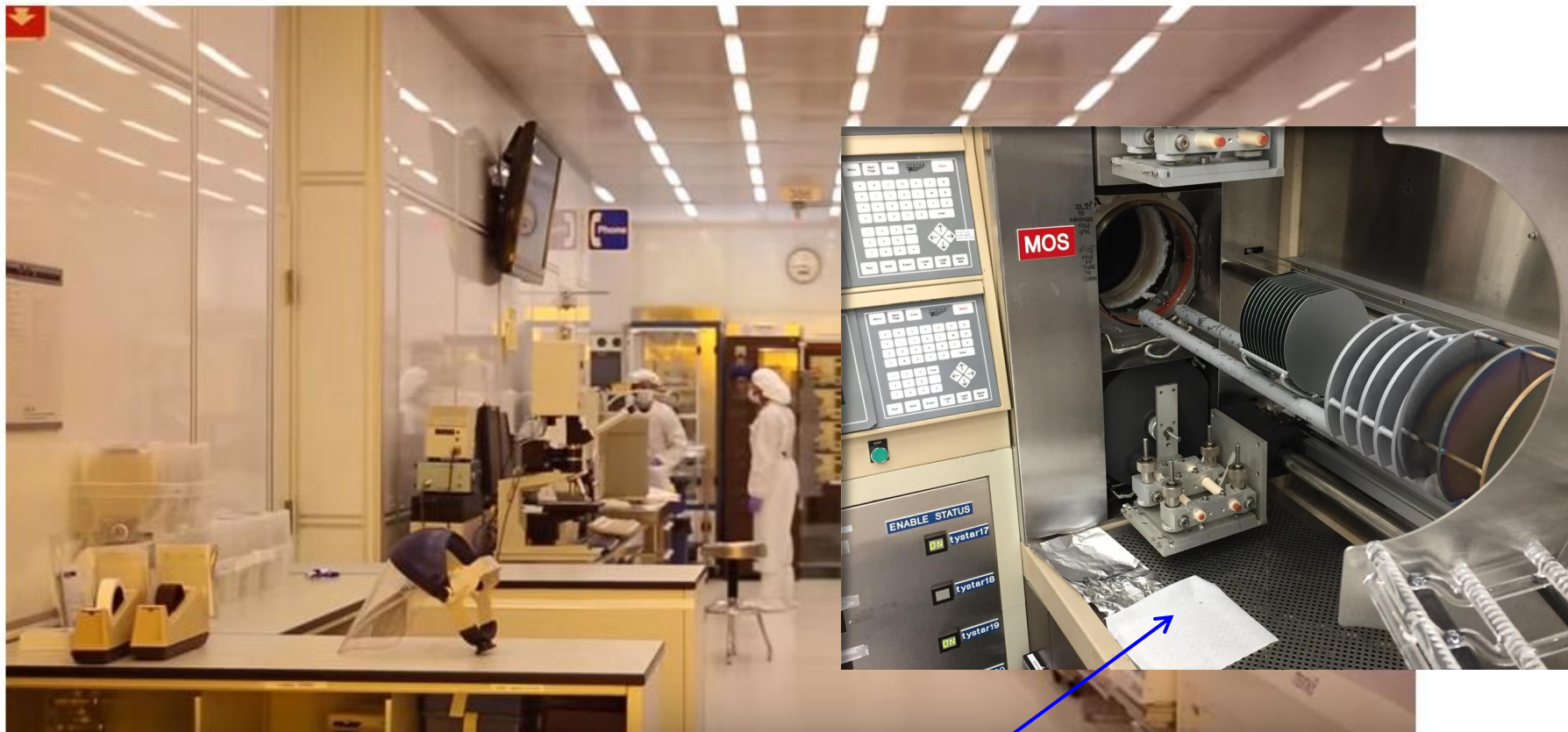
BULK LIFETIME	392 $\mu$ s
SRV	<10 cm/s.

Richard Ahrenkiel  
Lakewood Semiconductor



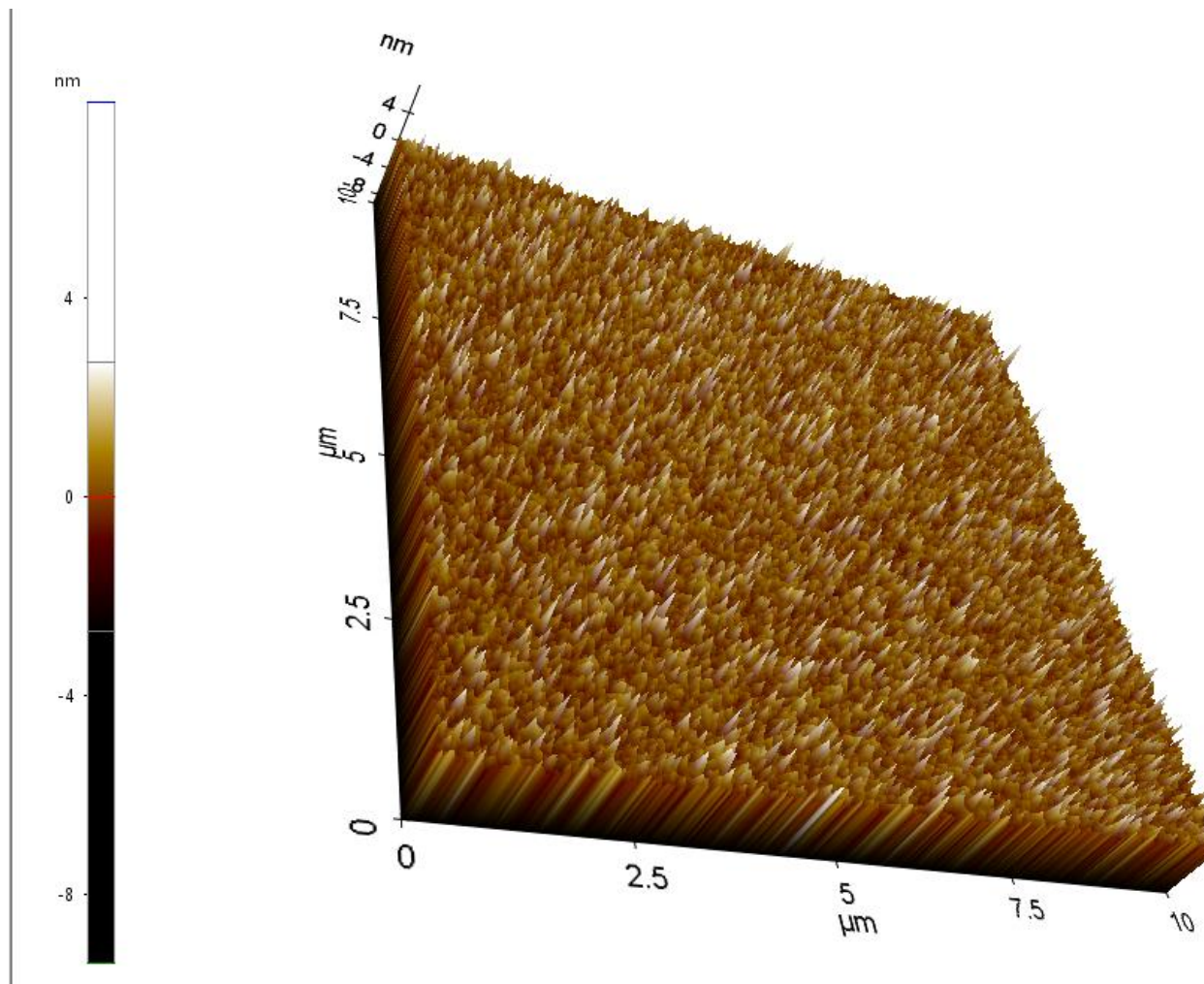
Photoconductive  
decay lifetime  
measurements

LNBL processing in  
progress



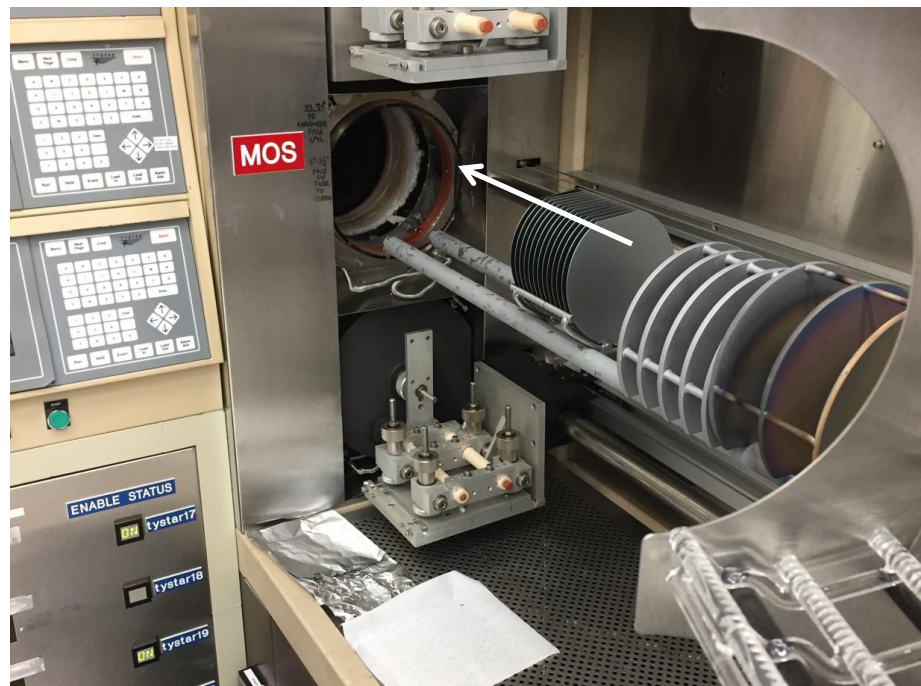
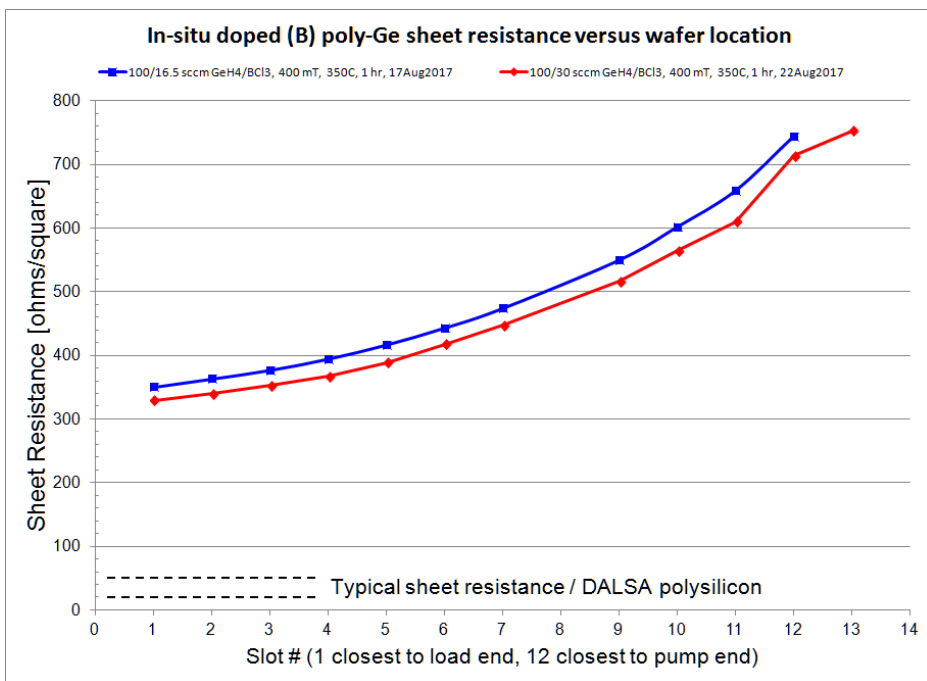
- Polycrystalline Ge (in-situ doped) capabilities
- Advanced characterization tools for the Ge technology development
  - Spectroscopic Ellipsometer and Atomic Force Microscopy
- Deep UV wafer stepper (250 nm lines / spaces) and TCP polysilicon etcher
- Atomic layer deposition

- Atomic Force Microscopy study
  - $\text{SiO}_2\text{-GeO}_2\text{-Ge}$  gate stack fabricated in the MSL



# LPCVD Ge investigations



- Interest in an in-situ doped poly-Ge film that could be deposited at  $\sim 350^\circ\text{C}$  / possible gate electrode
- Sheet resistance high and variable across the chamber despite numerous attempts varying the  $\text{BCl}_3$  to  $\text{GeH}_4$  ratio





# LPCVD Ge investigations

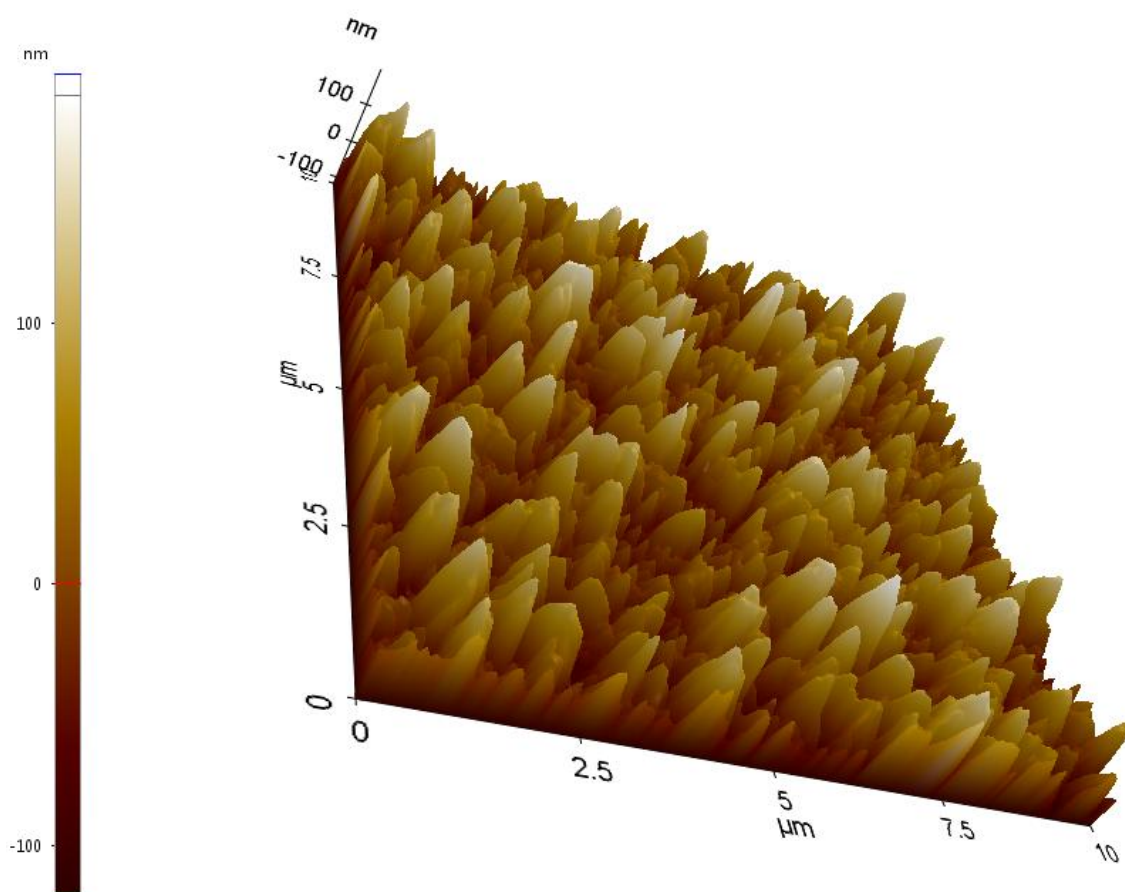
- Table below shows some results from Boron implantation and post-implant annealing

Sheet resistance in ohms/square	1 hr 350C	1 hr 375C	1 hr 400C	1 hr 425C
Process #1	2038K $\pm$ 9.5%	76.9 $\pm$ 219%	17.6 $\pm$ 2.2%	17.5 $\pm$ 1.1%
Process #2	1431 $\pm$ 33.9%	19.2 $\pm$ 131%	17.0 $\pm$ 0.83%	16.7 $\pm$ 0.85% 
Process #3	3500K $\pm$ 6.2%	1919K $\pm$ 7.0%	13.9 $\pm$ 3.5%	12.7 $\pm$ 1.2%
Process #4	10.0M $\pm$ 5.8%	5281K $\pm$ 7.4%	28.7 $\pm$ 9.5%	16.6 $\pm$ 0.55%
Process #5	95.4 $\pm$ 12.5%	22.7 $\pm$ 3.6%	20.9 $\pm$ 1.3%	

- Permission has been granted by the Nanolab staff to deposit polyGe films on Ge transistor wafers
- Plan to add this deposition capability to the MSL

# LPCVD Ge investigations

- LPCVD polyGe films:
  - More effort needed in terms of film flatness





# Lincoln Labs Ge CCD effort

- MIT Lincoln Laboratory has a long history of CCD production (Keck DEIMOS, PAN-STARRS, new TESS exoplanet satellite, latter two fully depleted CCDs)
- Initial Ge CCD report published Sept. 2015
- Advanced technologies (193 nm litho, high-k dielectrics, 200nm gaps)
  - Very open about the Ge issues they have observed
- Our approach is geared to possible tech transfer (DALSA)
  - Must demonstrate results

## Microelectronics Laboratory

LOCATION: MIT Lincoln Laboratory  
TOPIC: microelectronics  
R&D AREA: Advanced Technology

70,000 ft<sup>2</sup>  
MSL 700 ft<sup>2</sup>

The Microelectronics Laboratory is a state-of-the-art semiconductor research and fabrication facility that supports the design, fabrication, and packaging of novel devices.







# Summary

- Making progress with transistor fabrication with  $\text{SiO}_2\text{-GeO}_2$  gate insulators
  - Quite exciting to see the prior R&D efforts progressing from a hopeless water soluble film to that same film showing encouraging properties
- High-purity Ge effort well underway
- Looking forward to polyGe devices
- Prototype CCD layouts are included on the mask design / more technology development
- Implement cryogenic studies of test structures

**Special thanks to Co Tran / Expert on MSL processing and equipment**